A Framework for Precomputed and Captured Light Transport

JAAKKO LEHTINEN
Helsinki University of Technology, and Remedy Entertainment Ltd.

Several types of methods precompute or capture light transport operators in either virtual or real scenes. Precomputed radiance transfer methods interactively render realistic images of static scenes under dynamic incident illumination, while reflectance field techniques capture an appearance model of a real scene for relighting purposes. In this article we present a unifying mathematical framework for methods that precompute or capture light transport operators, and characterize a large body of earlier work in its terms. The framework is given in the form of an operator equation that extends the rendering equation to account for a constrained space of emissions. The connections between traditional global illumination methods and precomputed transfer techniques become apparent through the explicit equation. Based on insight provided by the unifying view, we outline possibilities for new methods, particularly the wider adaptation of previous, hierarchical finite element techniques for efficient computation of the transport operators.

Categories and Subject Descriptors: I.3.7 [**Computer graphics**]: Three-Dimensional Graphics and Realism

General Terms: Theory

Additional Key Words and Phrases: Precomputed light transport, precomputed radiance transfer, relighting, global illumination

ACM Reference Format:

Lehtinen, J. 2007. A framework for precomputed and captured light transport. ACM Trans. Graph. 26, 4, Article 13 (October 2007), 22 pages. DOI = 10.1145/1289603.1289604 http://doi.acm.org/10.1145/1289603.1289604

1. INTRODUCTION

Research in global illumination strives for fast rendering of realistic images of virtual scenes by simulating the propagation of light according to the ray-optics model. Most global illumination techniques solve the problem once for a given configuration of the scene and the light sources. In contrast, *relighting techniques* exploit the linearity of the light transport problem for precomputing solutions that are valid for a certain simple subspace of possible lighting conditions, as opposed to just a single lighting configuration. Here we mean by "simple" that the space is either low-dimensional or otherwise "small" in a sense to be made precise later. Such precomputed light transport operators allow fast runtime computation of illumination solutions for dynamic incident lighting that varies within the predetermined parameterization. Current methods support free-form reflectance and moving viewpoints, although preprocessing costs can be prohibitively high, and compression must be applied to the resulting data sets in order to keep consumption of runtime resources reasonable. On another front, capturing the light transport properties of real scenes has received a significant amount of attention. The essential goal is the same: Being able to render images of real scenes under novel lighting conditions, preferably from an arbitrary viewpoint.

Contributions. We present a simple but general mathematical framework for precomputed light transport in virtual scenes and light transport captured from real scenes. Our framework takes the form of an abstract linear operator equation that extends the well-known rendering equation. Using the framework, we show that precomputed radiance transfer, synthetic image relighting, and techniques that capture the light transport in a scene for relighting purposes (reflectance fields, environment matting, bidirectional texture functions) can all be described as realizations of the same fundamental principle. The framework enables us to clearly see the similarities between different methods, for both virtual and real scenes. The operator equation may be solved using a number of well-known numerical techniques. In particular, our formulation includes both forward and adjoint methods in a natural way. We discuss possible directions for future research in precomputed light transport based on the unified view, but present neither details on new techniques nor qualitative comparisons between those that have been previously published. In its way, this article aims to continue the tradition of formalizing light transport by describing a mathematical basis for a large body of diverse algorithms.

The article is structured as follows. In the rest of the introduction we cover background on global illumination and some methods used to approximately solve the illumination problem, and give an introduction to the adjoint formulation of light transport. In the second section we present a mathematical framework for precomputed transport. The framework takes the form of an abstract operator equation. The third section explains how previous techniques can be seen as special cases of the framework, and the fourth section is devoted to thoughts on future research based on the current state

This work has been supported in part by a NVIDIA fellowship, the National Technology Agency of Finland (TEKES), Anima Vitae, AMD Finland, NVIDIA Helsinki, Nokia, Remedy Entertainment, and the Helsinki Graduate School in Computer Science and Engineering.
Author's address: J. Lehtinen, P. O. Box 5400, Telecommunications Software and Multimedia, Helsinki University of Technology, FI-02015 TKK, Finland; email: jaakko@tml.hut.fi.

of the art. Due to the already large body of references in this text, some common terms and techniques are assumed to be common knowledge and are left without a proper citation. Our equations are always written for a single wavelength of light, and we deal with a nonparticipating medium, except for subsurface scattering specified by the BSSRDF model.

1.1 Background

Finite element global illumination methods approximate the distribution of light in the scene as linear combinations of basis functions defined on the space of surface appearance functions, that is, radiance distributions. The best-known of these are the radiosity method and a large collection of its variants. They are all based on the assumption that the surfaces are perfect Lambertian reflectors. Also view-dependent techniques for glossy reflectors exist [Immel et al. 1986; Sillion et al. 1991; Christensen et al. 1996], but they have not been widely used in applications. They are, however, clearly connected to recent glossy precomputed light transport methods. A finite element solution to the continuous rendering equation involves approximating the continuous light transport operator by a discretized one defined on the subspace where the solution is sought. This discrete representation is a matrix, and the solution of the linear system associated with it is a vector of coefficients that modulate the basis functions of the approximating subspace; the sum of the modulated basis functions is the approximate illumination solution. The right-hand side of the equation is a vector that describes the light emitted on the scene. As is the case with all global illumination algorithms, finite element techniques are computationally heavy. The dimension of the approximating subspace is in all cases of practical interest so large that numerical inversion of the matrix that defines the discrete problem is traditionally not attempted. Instead, the solution for a given (fixed) right-hand side is computed by iterative methods that start from the right-hand side and either iterate in a matrix-free way by evaluating single rows or columns of the matrix on-the-fly in a "gathering" or "shooting" operation, or use a hierarchical representation of the discrete transport matrix for fast evaluation of matrix-vector products. Nonhierarchical explicit construction of the matrix that defines the discretized problem is completely infeasible due to the huge number of degrees of freedom, which often runs in millions.

Global illumination methods that produce pictures by ray tracing do not involve a discretized transport operator. The solution they produce is a set of pointwise estimates of the lighting solution that are averaged to produce the image. Such methods, in their purest form, do not have any "global" knowledge of the lighting solution. There are, however, methods that speed up path tracing–like techniques by caching information in spatial data structures. The irradiance cache [Ward et al. 1988] and photon mapping [Wann Jensen 1996] are now-canonical examples. Also these methods render the solution anew if the emission function changes.

As mentioned, traditional finite element global illumination methods do not invert the discrete transport operator, but use it in an iterative linear solver instead. But were we in possession of a true discretized inverse of the transport operator, we could have the lighting change in our scene and render relit pictures of it with little work. This is exactly what precomputed light transport essentially means: precomputing or capturing the discrete solution operator that turns an emitted radiance distribution into the corresponding outgoing lighting solution, including global illumination effects. Such techniques are able to render scenes in lighting conditions that change according to a predetermined parameterization, without requiring a new preprocessing step for each lighting configuration. The key enabling insight is that the space of possible emissions can often be constrained to be much smaller than the subspace used for representing lighting solutions, either in the sense that it is low-dimensional, or that it is easy to represent linear functionals (reflectance functions) on it due to its simple geometry. This makes the computation and representation of the solution operator much easier than in the case of traditional finite element methods. The same idea of explicitly capturing the light transport operator for a scene is behind methods that relight real scenes. These techniques include surface reflectance fields, environment matting and bidirectional texture functions. They too avoid the excessive size of the transport matrix by constraining the lighting to lie in some simple subspace of all possible lighting conditions.

The mathematical framework that we present in Section 2 encompasses both synthetic relighting and methods based on capturing light transport in real scenes by defining a simple abstraction for the space of possible lighting conditions, and an operator that determines how light propagates from this emission space onto the scene.

1.2 Mathematical Tools for Global Illumination

This section presents a concise review of the subset of the equations associated with global illumination that will be used in the remainder of the article. The treatment is based on an operator formulation posed on linear spaces of functions. Such formulations have been studied extensively, for example, by Dutré [1996], Lafortune [1996], Veach [1997], and Pattanaik and Mudur [1995]. The reader with no previous familiarity with these concepts may want to consult these references or a textbook [Dutré et al. 2003; Cohen and Wallace 1993] before proceeding. Table I summarizes our notation.

1.2.1 *Radiance and the Rendering Equation.* Radiance is the quantity that describes the appearance of the surfaces of a scene: For each point and for each direction, it characterizes the amount of light that leaves or impinges upon a surface patch located at that point. We denote the radiance leaving a differential surface patch situated at x into direction ω by $L(x \rightarrow \omega)$, and the radiance incident upon a patch at x from direction ω by $L(x \leftarrow \omega)$. We denote the set of the surfaces in the scene by S and the sphere of directions by Ω. The linear vector space of radiance functions on the scene is denoted by $\mathbb{X} = \mathbb{X}(S \times \Omega)$; that is, each radiance function $L \in \mathbb{X}$ is a function of position and direction. We allow both outgoing and incident functions to exist in the same space in order to avoid notation bloat. The incident or outgoing nature of a function is always clear from the context.

The rendering equation [Kajiya 1986] describes the equilibrium distribution of radiance within a scene. It can be written in an abstract form as

$$L = \mathcal{T}L + E,$$

where L is the unknown lighting solution, $\mathcal{T}$ is the so-called transport operator, and E is the emitted radiance function that defines the light sources. The exact form of the operator $\mathcal{T}$ depends on the geometry and the reflective properties of the scene, but it is always a linear integral operator that that maps a given radiance distribution function L into a new function $(\mathcal{T}L)$, through one reflection. Also subsurface scattering can be accounted for via the BSSRDF model. Since by linearity $L = \mathcal{T}L + E \Leftrightarrow (\mathcal{I} - \mathcal{T})L = E$, where $\mathcal{I}$ is the identity mapping, the formal solution to the global illumination problem may be written as

$$L = (\mathcal{I} - \mathcal{T})^{-1}E = \mathcal{S}\,E \tag{1}$$

Table I. The Notation Used in this Article

$L(x \rightarrow \omega)$	Radiance leaving x towards ω
$L(x \leftarrow \omega)$	Radiance impinging upon x from direction ω
$E(x \rightarrow \omega)$	Radiance emitted from x towards ω
$E(x \leftarrow \omega)$	Radiance emitted towards x from direction ω
$\mathbb{E}$	Emission space
$\mathbb{E}_h$	Finite-dimensional subspace of $\mathbb{E}$
Ω	The sphere of directions in 3D
S	The set of surface points in the scene
$\mathbb{X}(S \times \Omega)$	The space of radiance functions on the scene
$\mathbb{X}_h$	A finite-dimensional subspace of $\mathbb{X}(S \times \Omega)$
$\mathcal{T}$	Radiance transport operator
$\mathcal{T}_\mathrm{i}$	Radiance transport operator for incident radiance
$\mathcal{I}$	The identity mapping
$\mathcal{R}$	Local reflection operator, maps $L(x \leftarrow \omega)$ to $L(x \rightarrow \omega)$
$\mathcal{M}$	Measurement operator $\mathbb{X}(S \times \Omega) \mapsto \mathbb{R}^m$
$\mathcal{M}_x$	Subset of $\mathcal{M}$ that contains measurements associated with point x
$\mathcal{V}$	Initial transport operator $\mathbb{E} \mapsto \mathbb{X}(S \times \Omega)$
$\mathcal{S}$	$(\mathcal{I} - \mathcal{T})^{-1}$, the solution operator
$\mathcal{S}_\mathrm{i}$	$(\mathcal{I} - \mathcal{T}_\mathrm{i})^{-1}$, the incident solution operator
$\mathcal{P}$	Projection $\mathbb{X}(S \times \Omega) \mapsto \mathbb{X}_h$
$\mathcal{M}\mathcal{R}\mathcal{S}_\mathrm{i}\mathcal{V}$	Compound transport operator (matrix)
$\mathcal{P}\mathcal{S}_\mathrm{i}\mathcal{V}$	Incident transport operator (matrix)
m_i, m_i^*	The ith measurement functional in $\mathcal{M}$ and its adjoint solution
$\langle \ell, L \rangle$	Inner product of ℓ and L
Bold matrices, e.g., $\boldsymbol{T}_\mathrm{i}$	Finite element representations of continuous operators
$\boldsymbol{e}$, e_j, etc.	A vector and its jth component
$r(x, \omega)$	Ray casting function, returns closest point to x in direction ω

where the solution operator $\mathcal{S} := (\mathcal{I} - \mathcal{T})^{-1}$ is the inverse of the operator $(\mathcal{I} - \mathcal{T})$. This is a nondiscrete equation, meaning that all the operators are infinite-dimensional, which corresponds (roughly) to square matrices with an infinite number of entries. It is impossible to find a closed-form solution to the rendering equation in almost any case of interest, and thus only approximate solutions can be computed. To obtain them, either the equation must be discretized using a suitable method, for instance finite elements, or solutions must be approximated by computing pointwise numerical estimates by Monte Carlo methods. The inverse operator may be written as the infinite Neumann series

$$\mathcal{S} = \mathcal{I} + \mathcal{T} + \mathcal{T}^2 + \cdots \tag{2}$$

The local reflection operator $\mathcal{R}$ [Arvo et al. 1994] turns an incident radiance distribution defined over the surfaces and incident directions into an outgoing radiance function, again defined over the surfaces and outgoing directions, without propagating the light away from the surface. In the case of an opaque surface this corresponds to merely integrating the incident radiance at each surface point against the BRDF and the incident cosine factor for each outgoing direction. The operator can also be extended to model refraction [Heckbert 1991].

In the subsequent sections we will make use of *incident global illumination solutions*. The rendering equation is usually, as earlier, written using outgoing radiance as the unknown function, but an equivalent formulation can be written for incident radiance instead:

$$L_\mathrm{i}(x \leftarrow \omega) = E(x \leftarrow \omega) + (\mathcal{T}_\mathrm{i} L_\mathrm{i})(x \leftarrow \omega), \tag{3}$$

where $E(x \leftarrow \omega)$ is the radiance emitted towards x from direction ω, and $\mathcal{T}_\mathrm{i}$ is a transport operator defined on incident radiance functions. Here the subscript in L_i denotes the incident nature of the radiance function. In words, the radiance incident to x is the sum of radiance emitted and reflected towards x. An outgoing radiance solution can be computed from the incident solution simply by applying the local reflection operator $\mathcal{R}$ to it. The solution operator $\mathcal{S}_\mathrm{i}$ for the incident problem is defined analogously to the outgoing formulation.

1.2.2 *Finite Element Methods (FEM).* Finite element methods form a linear, finite-dimensional subspace $\mathbb{X}_h$ of the space of all possible radiance functions, and approximate the solution of the rendering equation by functions in this subspace. This amounts to looking for the solution as a linear combination of *basis functions*. After choosing the appropriate basis, application of, for example, the Galerkin or point collocation method [Atkinson 1997] leads to a finite-dimensional linear system

$$\boldsymbol{l} = \boldsymbol{T}\,\boldsymbol{l} + \boldsymbol{e} \quad \Leftrightarrow \quad \boldsymbol{l} = (\boldsymbol{I} - \boldsymbol{T})^{-1}\boldsymbol{e} \tag{4}$$

or equivalent. Here $\boldsymbol{l}$ and $\boldsymbol{e}$ are vectors of coefficients that identify the discrete solution and the projection of the emission function in the finite-dimensional approximating subspace $\mathbb{X}_h$, and $\boldsymbol{I}$ and $\boldsymbol{T}$ are matrices of size $\dim \mathbb{X}_h \times \dim \mathbb{X}_h$. The matrix $\boldsymbol{T}$ is a discretized version of the continuous transport operator $\mathcal{T}$. Notice that the emission vector is defined on the same space as the approximate solution.

1.2.3 *Measurements and Adjoints.* A measurement is a linear operation that acts on a function and produces a number. Evaluation of the value of the function at a certain (fixed) point is an example; computing its average by integration is another. Many tasks in rendering can be formulated by linear measurements. The canonical example is determining the color for a pixel. The radiance flowing through the pixel onto the imaging sensor is integrated with a sampling filter that produces a real number for each color band in consideration. Projection of a radiance function into a finite-dimensional function space by integrating it against the dual basis is another example. Just as knowledge of the illumination solution is required only for those rays that fall within the support of a pixel filter when rendering an image, computing a single projection coefficient for the radiance functions has no use for illumination elsewhere except under the support of the corresponding dual basis function. We also note that asking for a point value of the illumination solution at a particular point and outgoing direction corresponds to measuring the solution by a Dirac impulse.

Any linear measurement of a function L can be stated as applying some *linear functional* ℓ to L. For our purposes, linear functionals are "measurement kernels" that one integrates against the function being measured according to

$$\langle \ell, L \rangle = \int_S \int_\Omega \ell(x, \omega)\, L(x, \omega)\, \max(0, \cos\theta)\, dA_x\, d\omega, \tag{5}$$

where θ is the angle between the surface normal of the patch dA_x and ω. $\langle \ell, L \rangle$ is called the inner product of ℓ and L. To make a measurement of the illumination solution, we need the radiance field in the scene, that is, the solution of the rendering equation. This is written as

$$r = \langle \ell, L \rangle = \langle \ell, \mathcal{S}E \rangle\,,$$

where we denote the value of the measurement by r, $\mathcal{S}$ is the solution operator of the global illumination problem, and ℓ is the pixel sampling filter defined on the space of radiance functions. Now, to each linear operator $\mathcal{T} : A \mapsto B$ that maps a function from an inner product space A to another inner product space B (notice that A

and B can also coincide) there exists an *adjoint operator* $\mathcal{T}^*$ that satisfies

$$\langle y, \mathcal{T}x\rangle_B = \langle \mathcal{T}^* y, x\rangle_A \tag{6}$$

for all $x \in A$ and $y \in B$. Thus, the adjoint operator works in the opposite direction; that is, $\mathcal{T}^* : B \mapsto A$. Here we have denoted the space on which the inner product operates by the subscript after the closing wedge. The exact form of the adjoint operator depends on the inner product, but determining the exact formulae for adjoint operators is (at least usually) possible through simple manipulation of the expression for the "forward" inner product $\langle y, \mathcal{T}x\rangle$. The typical uses of adjoint operators in global illumination are such that $A = B$, but we make use of the more general form later. An intuitive understanding of the duality between a linear operator and its adjoint can be obtained by considering matrices in $\mathbb{R}^n$: There the adjoint of a matrix is its transpose.

Adjoint equations provide a framework for computing linear measurements efficiently. Intuitively, just as we can start from the emission E, solve the rendering equation to get L, and then measure L by ℓ, we can go the other way around and start from the measurement function ℓ, solve an *adjoint equation* to get an *adjoint solution* ℓ^*, and measure the emission E by ℓ^*, formally

$$r = \langle \ell, L\rangle = \langle \ell, \mathcal{S}E\rangle = \langle \mathcal{S}^*\ell, E\rangle = \langle \ell^*, E\rangle\,, \tag{7}$$

where $\ell^* := \mathcal{S}^*\ell$, and the second-last equality is due to Equation (6). To gain intuition on $\mathcal{S}^*$, consider the Neumann series from Equation (2). The linearity of the adjoint and the series on the right-hand side suggest that

$$\mathcal{S}^* = (\mathcal{I} + \mathcal{T} + \mathcal{T}^2 + \ldots)^* = \mathcal{I} + \mathcal{T}^* + \mathcal{T}^*\mathcal{T}^* + \cdots$$

It follows that the adjoint solution can be computed by transporting the original functional ℓ bounce by bounce in the scene. The measurement travels to the opposite direction as light. The efficiency of the adjoint formulation stems for the fact that propagating the measurement functional in the scene using the adjoint can be done in a fashion where computational resources are only spent in calculations that are guaranteed to affect the value of the measurement. In contrast, a forward method that first solves for the illumination L needs to resolve the illumination everywhere before the measurement can be computed. Forward and adjoint operations can be combined to bidirectional algorithms such as bidirectional path tracing. See the survey of Christensen [2003] and the references therein for an in-depth discussion.

Much of the global illumination literature treats the measurement functionals as "importance." The adjoint solutions that correspond to the measurement functionals are seldom computed explicitly; rather, most techniques compute the inner products that determine the *values* of the measurements on a particular lighting solution. Explicit computation of importance solutions is employed in some finite element methods for driving the refinement of transport interactions for regions that are important to the final image [Smits et al. 1992; Christensen et al. 1996], and in some particle tracing methods for guiding the storage and reflection of photons, for example, Peter and Pietrek [1998]. However, the importance solution is in both cases a mere byproduct. In contrast, we will be interested in explicitly computing and storing the adjoint solutions, because knowledge of the adjoint solution allows the computation of the values of measurements with changing illumination (see Equation (7)). Interestingly, the bidirectional radiosity technique of Dutré et al. [1996] computes explicit importance solutions for individial surface patches in the radiosity setting, but the authors do not use them for relighting purposes.

2. A FRAMEWORK FOR PRECOMPUTED AND CAPTURED LIGHT TRANSPORT

This section describes a mathematical framework for methods that either precompute or capture a light transport operator and use it to relight pictures or scenes. The key ingredients of the framework are the *emission space* $\mathbb{E}$ and the *initial transport operator* $\mathcal{V}$. The emission space $\mathbb{E}$ is a linear function space defined on a simple manifold, such as the sphere of directions in the case of distant illumination. The functions that belong to this space represent the light emitted onto the scene. The initial transport operator $\mathcal{V}$ maps emission functions from $\mathbb{E}$ onto direct incident radiance functions on the scene. An ordinary light transport solution operator then takes over and turns this incident lighting into a global illumination solution, after which the solution is measured by some finite number of measurement functionals that usually either produce a picture of the scene or project the illumination solution into some finite function space to produce an approximation of the appearance of the scene. The concatenation of all these operators defines a compound transport operator that takes the incident lighting function from $\mathbb{E}$ into some finite set of measurements of the corresponding illumination solution. After a finite representation of this compound operator has been precomputed or acquired, it may then be used for efficient relighting of the scene. This solution operator is more manageable than the full discretized inverse of the global illumination problem. This is either because the emission vectors that it transforms to illumination solutions are shorter (if the emission space is low-dimensional), or because the adjoint solutions that correspond to each measurement can be approximated efficiently due to the simplicity of $\mathbb{E}$, or both. *The goal of precomputed and captured light transport is to obtain these operators either by simulation or measurement.* As we will show in the subsequent section, this abstract framework describes most methods that precompute light transport by suitable choices of the space $\mathbb{E}$, the operator $\mathcal{V}$, and how the solutions are measured. It also enables us to give an explicit mathematical reasoning for methods that approximate the adjoint solutions that correspond to each of the measurements.

We begin by discussing the emission space and initial transport operator in Sections 2.1 and 2.2. After presenting the transport operator equation in Section 2.3, we also describe a factored version of it (Section 2.4), where the solution operator produces a discretized incident illumination solution on the scene, which is then operated on by final reflection operators that can be shared between many surface points. We also treat the finite element discretization of the transport equations (Section 2.5), and conclude in Section 2.6 with thoughts on methods for computing and representing the transport operators based on adjoint equations.

2.1 The Emission Space

We define the emission space $\mathbb{E}$ as the linear function space that contains all possible emission functions. The functions are real-valued, and they are defined on some manifold, which we call the "underlying manifold" or the "emission manifold." For example, distant illumination falling on the scene is represented by a spherical function. In this case the underlying manifold is the sphere of directions Ω, and the emission space $\mathbb{E}$ is the infinite-dimensional linear space of all (suitably well-behaved) functions defined on it. For another example, consider N fixed local light sources, and denote by S_L the set of surface points on the light sources. Now the emission manifold is $S_L \times \Omega$, and the function space $\mathbb{E}$ is the subspace of $\mathbb{X}(S \times \Omega)$ that contains functions that are nonzero only on S_L.

In many cases we will also focus on some finite-dimensional subspace $\mathbb{E}_h$ of the emission space. Such subspaces are spanned by collections of a finite number of basis functions defined on the base manifold. As $\mathbb{E}$ is a linear function space, we are free to choose a basis of our liking to represent the emission functions. For example, a finite set of spherical harmonics defines such a finite-dimensional subspace of all spherical functions. Spherical functions may also be discretized by some (fixed) set of directional light sources (this is a "basis of Dirac impulses"), or by using a cube map of fixed resolution, which corresponds to using either a piecewise constant basis with disjoint basis functions or a bilinear basis that consists of "hat" functions. Many techniques employ wavelet bases defined on the cube map parameterization. If N fixed local light sources have fixed emission patterns, an interesting finite-dimensional subspace $\mathbb{E}_h$ is the linear span of those patterns.

The simplicity of the emission manifold is important because we will later need to represent linear functionals on $\mathbb{E}$. If the manifold is simple, such as the sphere of directions, approximation and representation of the functionals is easier. These functionals are "reflectance functions" in the parlance of several relighting methods.

The definition of the emission space alone does not enable us to render illumination solutions on the scene. For that purpose we need to introduce a mapping from $\mathbb{E}$ onto incident radiance functions on the scene, so that an illumination solution operator defined on the space $\mathbb{X}$ of radiance functions on the scene can take over and produce a global illumination solution that corresponds to the emission specified on $\mathbb{E}$.

2.2 The Initial Transport Operator

The initial transport operator $\mathcal{V}$ maps functions from the emission space $\mathbb{E}$ to the corresponding direct incident illumination functions on the scene. Intuitively, it answers the question "given that my emission function is $E \in \mathbb{E}$, what is the resulting direct incident radiance distribution $E(x \leftarrow \omega)$ on the scene?" Formally, we define $\mathcal{V}$ as a linear mapping from the emission space to the space of incident radiance functions on the scene, that is, $\mathcal{V} : \mathbb{E} \mapsto \mathbb{X}(S \times \Omega)$. The rationale for the symbol $\mathcal{V}$ is that in the simplest cases $\mathcal{V}$ corresponds merely to a multiplication of the emission function by the function that describes visibility between points on the emission manifold and points on the scene. Figure 1 illustrates how the initial transport operator $\mathcal{V}$ maps lighting functions from the emission space onto the scene, and how its adjoint $\mathcal{V}^*$ transfers measurement functionals from the scene onto the emission space.[1] It is essential that the relationship of the emission variables to the corresponding radiance distributions is linear, that is, that $\mathcal{V}$ is indeed a linear operator. Unfortunately, this requirement rules out some parameterizations. For instance, the position of the sun in the sky for a particular geographic location may obviously be parameterized by just one variable. However, the irradiance cast by the sun onto a particular surface location on the ground is clearly not linear with respect to time: One cannot compute the irradiance at twelve o'clock by multiplying the irradiance from six o'clock by two.

An intuitive picture of $\mathcal{V}$ and its relationship to the emission space is offered by the following simple examples. First, consider a scene lit by a distant spherical lighting environment, for example, skylight. Here the emission space contains all (suitably well-behaved) functions that are defined on the sphere Ω. By our definition of the initial transport operator, the direct incident lighting on the scene due to the emission function in $\mathbb{E}$ is given by $\mathcal{V}E$, and due to simple geometric considerations

$$E(x \leftarrow \omega) = (\mathcal{V}E)(x, \omega) = E(\omega)\, V(x, \omega), \tag{8}$$

that is, the operator $\mathcal{V}$ corresponds to a pointwise multiplication of the emission function by the visibility function $V(x, \omega)$ that encodes by value 1 the directions where the point x can see the distant sphere and by 0 the directions that are occluded. Deriving the expression for $\mathcal{V}$ in the case of fixed local light sources is just as simple by defining a new visibility function $V_L(x, \omega)$ that has value 1 if the point seen from x in direction ω belongs to a light source and 0 otherwise.

It is clear from the above that $\mathbb{E}$ and $\mathcal{V}$ may well be designed to contain both distant environmental light and local light sources. Also, nothing prevents utilizing locally defined spatial function bases—indeed, some local precomputed transport techniques work this way [Kristensen et al. 2005; Kontkanen et al. 2006; Hašan et al. 2006]. The form of the resulting operator $\mathcal{V}$ is straightforward in all cases. Note that these examples by no means form an exhaustive list of all possible emission spaces and initial transport operators. As a general rule, the operator $\mathcal{V}$ is (as in the preceding) defined by the visibility function that encodes the visibility between points in the emission manifold and points on the scene. In addition, it must account for any geometric factor that describes how light from the point in the domain of $\mathbb{E}$ is transformed to radiance at the scene point.

2.3 The Operator Equation for Precomputed and Captured Light Transport

Using the emission space and initial transport operator introduced above, we are now ready to piece together the operator equation for precomputed light transport. We use the incident form of the rendering equation, because we will introduce a split between the final reflection step and the incident solution in the next section. We repeat the rendering Equation (3) for incident radiance L_i here for convenience:

$$L_\mathrm{i} = \mathcal{T}_\mathrm{i} L_\mathrm{i} + E_\mathrm{i}; \quad \text{that is,} \quad L_\mathrm{i} = \mathcal{S}_\mathrm{i} E_\mathrm{i}.$$

Here $E_\mathrm{i} = E(x \leftarrow \omega)$ is the emitted radiance directly incident upon x and $\mathcal{S}_\mathrm{i}$ is the solution operator that maps an incident distribution E_i into the solution of the global illumination problem. Note that $\mathcal{S}_\mathrm{i}$ may include any linear form of light transport. Now, due to the way we defined $\mathcal{V}$, this is just

$$L_\mathrm{i} = \mathcal{S}_\mathrm{i} \mathcal{V} E, \tag{9}$$

so that the emission is now given as a function $E \in \mathbb{E}$ in the emission space, and $\mathcal{V}E$ defines the incident radiance function due to E on the scene. The equation is similar in form to the rendering equation for incident radiance; the only difference is that the emission function

[1] As an example we derive the formula for the adjoint $\mathcal{V}^*$ in the case of distant environmental illumination. Other cases can be derived in a similar fashion. Looking back to Equation (6), the adjoint operator is defined by the relation $\langle \ell, \mathcal{V}E \rangle_{\mathbb{X}} = \langle \mathcal{V}^* \ell, E \rangle_{\mathbb{E}}$ for all emissions E and linear functionals ℓ. It is easy to tease out an explicit formula by expanding the inner product, reordering integrations and rearranging factors:

$$\begin{aligned}
\langle \ell, \mathcal{V}E \rangle_{\mathbb{X}} &= \int_S \int_\Omega \ell(x, \omega)\, (\mathcal{V}E)(x, \omega)\, \cos\theta \, dA_x \, d\omega \\
&= \int_S \int_\Omega \ell(x, \omega)\, E(\omega) V(x, \omega) \cos\theta \, dA_x \, d\omega \\
&= \int_\Omega E(\omega) \left[\int_S \ell(x, \omega)\, V(x, \omega) \cos\theta \, dA_x \right] d\omega \\
&= \langle \mathcal{V}^* \ell, E \rangle_{\mathbb{E}}, \quad \text{with} \\
(\mathcal{V}^* \ell)(\omega) &:= \int_S \ell(x, \omega)\, V(x, \omega)\, \cos\theta \, dA_x .
\end{aligned}$$

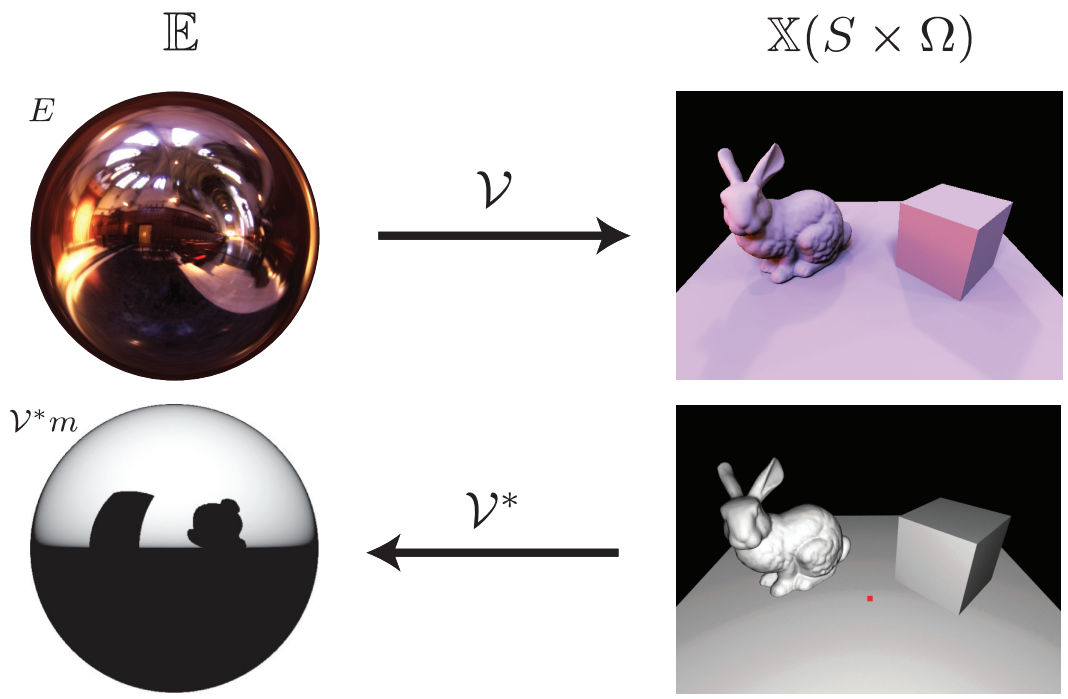

Fig. 1. Illustration of the initial transport operator $\mathcal{V}$ and its adjoint $\mathcal{V}^*$ for distant illumination. **Top row**: The initial transport operator $\mathcal{V}$ maps lighting functions from the emission space $\mathbb{E}$ onto the space $\mathbb{X}(S \times \Omega)$ of incident radiance functions on the scene. The incident irradiance on the scene due to the distant lighting environment E is illustrated on the right (i.e., the 4D incident radiance function $(\mathcal{V}E)(x \leftarrow \omega)$ has been integrated with the local cosine term for each pixel for visualization). **Bottom row:** The adjoint operator $\mathcal{V}^*$ maps measurement functionals from the scene onto the emission space. Here, a functional m that measures the irradiance incident onto the point marked in red in the right image is transported by $\mathcal{V}^*$ onto the emission space. The resulting function $\mathcal{V}^* m$ on $\mathbb{E}$ indicates how light from different points on the emission manifold (different directions in this case) affect the direct irradiance at the red point. Note that the irradiance at the corresponding pixel on the upper-right image is obtained by computing the inner product of the emission function and $\mathcal{V}^* m$.

is determined from the function E by $\mathcal{V}$. The above immediately reduces to the usual rendering equation for incident radiance if the emission space is taken to be the same as the space of radiance distributions on the scene, since in this case $\mathcal{V} = \mathcal{I}$. This case can also be interesting in the context of precomputed transport [Kontkanen et al. 2006].

In order to render pictures, the outgoing radiance must be determined for points on the scene. This is accomplished by applying the local reflection operator $\mathcal{R}$ to the incident solution. This results in the equation

$$L = \mathcal{R}\mathcal{S}_{\mathrm{i}}\mathcal{V}\,E, \tag{10}$$

which is still infinite-dimensional in the sense that its solution L cannot be described using any finite number of parameters, regardless of the dimensionality of the emission space. Although we will apply a discretization to the operator $\mathcal{R}\mathcal{S}_{\mathrm{i}}\mathcal{V}$, it is also instructive to look at it in its nondiscretized form. It is clearly an integral operator, since it is a concatenation of two integral operators and $\mathcal{V}$, which is essentially a multiplication operator. Since it maps functions from $\mathbb{E}$ to $\mathbb{X}$, its *kernel* $\boldsymbol{t}(l, x, \omega)$ is a function on the Cartesian product of the emission manifold and $S \times \Omega$. Intuitively, the kernel describes how light from a single point in the emission manifold affects the illumination on the scene, including global illumination effects. Formally, outgoing radiance is obtained by integrating the product of the kernel and the emission function over the emission manifold (e.m.):

$$L(x \to \omega) = \int_{\text{e.m.}} \boldsymbol{t}(l, x, \omega)\, E(l)\, dl. \tag{11}$$

Here l is a point in the emission manifold. (Note that it need not be a two-dimensional point: For instance, if the emission space contains spatially and directionally varying emission functions, the points are four- or five-dimensional.) The kernel may be regarded as a direct generalization of the global reflection distribution function (GRDF) introduced by Lafortune and Willems [1994], which is in essence the kernel of the solution operator of the "usual" global illumination problem. Note that a similar argument holds for the kernel of the operator $\mathcal{S}_{\mathrm{i}}\mathcal{V}$ that does not include the final reflection. Interestingly, the "reflectance field" as defined by Debevec et al. [2000] also corresponds directly to this kernel function (cf. Section 3.2.3).

In order to get a finite result, a picture, say, we apply the measurement operator $\mathcal{M} : \mathbb{X} \mapsto \mathbb{R}^m$ that performs m linear measurements of the outgoing solution L. This yields the final equation (the "transport operator equation")

$$\boxed{\boldsymbol{r} = \left(\mathcal{M}\mathcal{R}\mathcal{S}_{\mathrm{i}}\mathcal{V}\right) E} \tag{12}$$

where $\boldsymbol{r} \in \mathbb{R}^m$ is the resulting vector of measurements. This equation is the crux of the present framework: The *compound transport operator* $\mathcal{M}\mathcal{R}\mathcal{S}_{\mathrm{i}}\mathcal{V}$ describes the mapping of an emission function

from the emission space onto a finite set of measurements of the lighting solution that corresponds to the emission. The form of this equation directly fits many applications. The measurement operator in the end can account for both integration of outgoing radiance against pixel sampling filters and projection of the outgoing radiance into a finite function basis, i.e., the vector $\boldsymbol{r}$ can represent a picture or an illumination solution discretized in terms of a function basis. In all cases $\mathcal{M}$ consists of a collection of measurement functionals $\{m_i\}_{i=1}^{m}$, so that r_i, the ith entry of the result vector, is computed by the inner product

$$r_i = \langle m_i, (\mathcal{R}\mathcal{S}_\mathrm{i}\mathcal{V})\, E\rangle_{\mathbb{X}}. \tag{13}$$

Thus, each row of $\mathcal{M}$ consists of a measurement functional. The operator may be pictured as a matrix with a finite number of rows and an infinite number of columns. In the case of image generation each of the m_i assume a nonzero value in the locations and directions of the scene that fall under the sampling filter associated with the ith pixel. Projection of the outgoing radiance into a function basis, on the other hand, requires computation of the inner products of the lighting solution and the corresponding dual basis functions. Now, it is clear that the dual basis functions can be taken to form the rows of $\mathcal{M}$, and the entry r_i of the result vector now denotes a coefficient by which the ith basis function is to be modulated when evaluating the approximate outgoing radiance.

The compound transport operator is *semidiscrete* in the sense that it takes a possibly infinite-dimensional function E to a finite vector. Of course, if we consider the finite-dimensional subspace $\mathbb{E}_h$, the operator is a finite matrix, even though we need to account for the infinite-dimensional solution operator $\mathcal{S}_\mathrm{i}$ to compute its entries. (This is of course usually impossible to perfect accuracy.) To see what the entries of the matrix are, remember that each function in $\mathbb{E}_h$ can be written as a linear combination of the basis functions C_k. Now we immediately obtain

$$\boldsymbol{r} = (\mathcal{M}\mathcal{R}\mathcal{S}_\mathrm{i}\mathcal{V}) \sum_{k=1}^{\dim \mathbb{E}_h} e_k C_k \;=\; \sum_{k=1}^{\dim \mathbb{E}_h} e_k[(\mathcal{M}\mathcal{R}\mathcal{S}_\mathrm{i}\mathcal{V})C_k] \tag{14}$$

by the linearity of the compound transport operator. Here the vectors $(\mathcal{M}\mathcal{R}\mathcal{S}_\mathrm{i}\mathcal{V})C_k$ are measurements of the *basis solutions* that correspond to each basis function of $\mathbb{E}_h$; the entry jk of the matrix is thus simply $\langle m_j, \mathcal{R}\mathcal{S}_\mathrm{i}\mathcal{V}\, C_k\rangle$, the response of the jth measurement functional to the lighting solution computed using only the kth lighting basis function as an emitter. *Any* global illumination technique capable of computing the basis solutions will do. We call any precomputed light transport method that computes these basis solutions a forward method. See the top row of Figure 2 for an illustration of a basis function in $\mathbb{E}_h$ and its corresponding basis solution in the case of image relighting.

It is also possible to consider the transport operator from another perspective, namely that of the measurement functionals. Applying the definition of the adjoint operator from Equation (6) to the single measurement from Equation (13) yields

$$r_i \;=\; \langle m_i, (\mathcal{R}\mathcal{S}_\mathrm{i}\mathcal{V})\, E\rangle_{\mathbb{X}} \;=\; \langle (\mathcal{R}\mathcal{S}_\mathrm{i}\mathcal{V})^* m_i, E\rangle_{\mathbb{E}} \;=\; \langle m_i^*, E\rangle_{\mathbb{E}}, \tag{15}$$

where $m_i^* := (\mathcal{R}\mathcal{S}_\mathrm{i}\mathcal{V})^* m_i = \mathcal{V}^*\mathcal{S}_\mathrm{i}^*\mathcal{R}^* m_i$ is the *adjoint solution* defined on $\mathbb{E}$ that corresponds to the measurement functional m_i. Regardless of the dimension of $\mathbb{E}_h$, the adjoint solution is a (piecewise) continuous function on the emission manifold. Considering these adjoint solutions leads to a measurement-centric interpretation of precomputed light transport, where the finite basis of $\mathbb{E}_h$ is in a less pronounced role. We call a precomputed transport technique that computes adjoint solutions instead of the basis lighting solutions an adjoint method. The bottom row of Figure 2 illustrates an adjoint solution that corresponds to a single pixel in an image relighting context.

The compound transport operator $\mathcal{M}\mathcal{R}\mathcal{S}_\mathrm{i}\mathcal{V}$ is *global* in the sense that the measurement $\mathcal{M}$ operates on the full 4D outgoing radiance field. However, these measurements are often higly localized spatially. For instance, many precomputed radiance transfer methods seek directional basis coefficients of outgoing radiance at a discrete set of points on the scene, while image relighting techniques compute the radiance towards the camera from areas under projected pixel footprints. This motivates introducing notation that explicitly reveals the surface location that is associated with each of the measurements. We do this by splitting the measurement operator into parts, so that $\mathcal{M}_x$ denotes the local measurement operator that contains only the measurement functionals that depend only on the radiance at or near x. We denote the measurements associated with point x by $\boldsymbol{r}_x$.

2.4 Factoring the Compound Transport Operator into Incident and Outgoing Parts

Previous work in many global illumination contexts [Ward et al. 1988; Gershbein et al. 1994; Wann Jensen 1996; Sloan et al. 2003] has shown that solving first for the incident radiance or irradiance at sample points on the object can be more efficient than solving directly for outgoing radiance. This is because incident radiance often varies over the surfaces slower than outgoing radiance. The most typical example is a textured surface patch that is located far away from the rest of the scene. This motivates splitting the computation in two parts. First a precomputed transport operator maps the incident illumination from the emission space into a discretized incident global illumination solution on the scene. The discrete incident spherical radiance solution is subsequently interpolated across the surfaces, and the final surface interaction (reflection according to a BRDF, say) is computed at each point using the interpolated incident illumination solution. Since by assumption the incident radiance varies slower than outgoing radiance, the incident solution can be sampled spatially more coarsely than outgoing radiance. Moreover, since the final interaction only depends on light incident to the point in question locally, the data required to perform this integration can be shared between multiple surface points, for example, in the form of a repetitive texture map [Gershbein et al. 1994] or a bidirectional texture function [Sloan et al. 2003].

We introduce this split into our operator equation before the the final reflection and measurement step:

$$\boldsymbol{r}_x = (\mathcal{M}_x\mathcal{R})(\mathcal{S}_\mathrm{i}\mathcal{V})E \;=\; (\mathcal{M}\mathcal{R})_x(\mathcal{S}_\mathrm{i}\mathcal{V})E.$$

It should be noted that the final operation $(\mathcal{M}\mathcal{R})_x$ that turns the incident global illumination solution at x into a set of measurements is indeed local, as the local reflection operator $\mathcal{R}$ only depends on the radiance incident to x, and by our assumption the measurement operator $\mathcal{M}_x$ also does not involve outgoing radiance from elsewhere. This justifies our notation $(\mathcal{M}\mathcal{R})_x$.

In order to exploit the split computationally, it is necessary to discretize the incident illumination solution. Otherwise we cannot get a finite representation for $(\mathcal{M}\mathcal{R})_x$, which is necessary for being able to precompute and use the operators efficiently at runtime. This discretization amounts to expressing the spatially varying incident illumination solution in a finite directional basis at each x. In order to be able to subsequently share the operators $(\mathcal{M}\mathcal{R})_x$ between different surface points, this directional basis needs to be the same over the whole scene, and moreover oriented with the local coordinate frame of the surface. This is achieved conveniently by expressing the incident solution using the tensor product of a spatial and

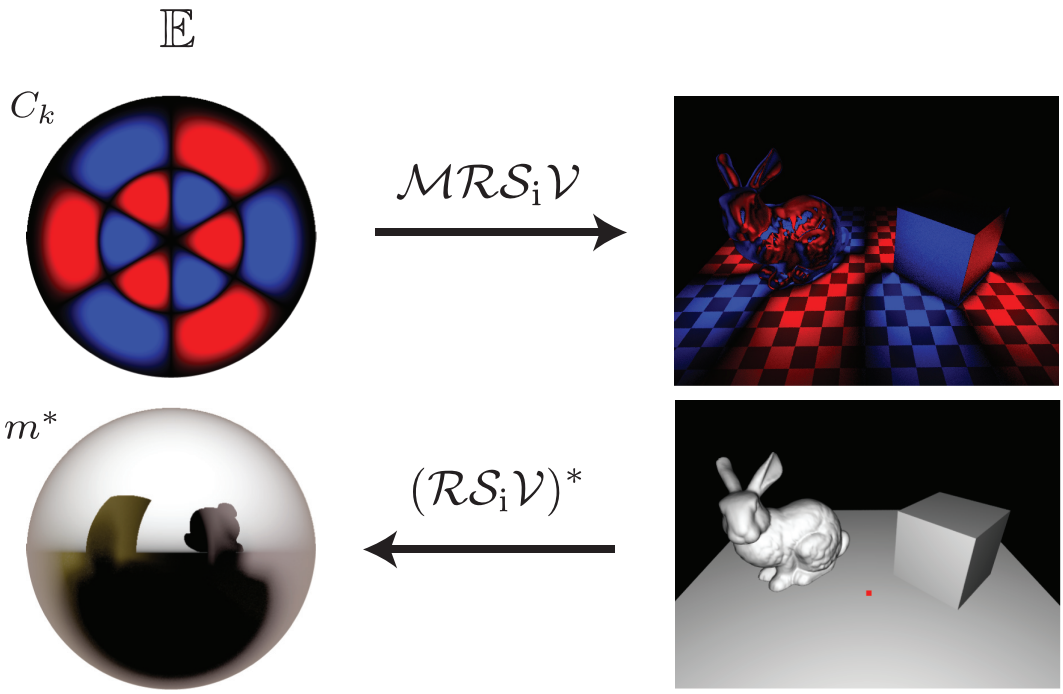

Fig. 2. Forward and adjoint solutions illustrated for image relighting with distant illumination. Both solutions have been computed by path tracing with one indirect bounce. **Top row**: A single basis function C_k of $\mathbb{E}_h$ is turned into a basis solution by the operator $\mathcal{MRS}_\mathrm{i}\mathcal{V}$. The image on the right corresponds to a single column of the transport matrix when using a fixed basis for $\mathbb{E}_h$ (see Equation 14). A single spherical harmonic is used for illustration so that red denotes positive and blue negative values. **Bottom row**: A pixel measurement functional m is turned into an adjoint solution m^* by the adjoint solution operator $(\mathcal{RS}_\mathrm{i}\mathcal{V})^*$. Note how indirect illumination reaches the pixel from directions that are occluded by the box and the bunny (compare to Figure 1). The brownish color is due to interreflection from the bunny (see Figure 3 right). The adjoint solution for a point measurement corresponds to the kernel function $\boldsymbol{t}(l, x, \omega)$ of the adjoint solution operator for fixed x, ω and varying l (see Equation 11).

directional basis, and applying a rotation to align the incident radiance to the local frame before the directional projection. Intuitively, the tensor product construction means that the spatial basis functions are used for approximating directional basis coefficient vectors over the surfaces. Projecting to the finite basis is denoted by the operator $\mathcal{P} : \mathbb{X}(S \times \Omega) \mapsto \mathbb{X}_h$, where $\mathbb{X}_h$ is the finite-dimensional approximating subspace. Applying the projector yields

$$\boxed{\boldsymbol{r}_x \approx (\mathcal{MR})_x(\mathcal{PS}_\mathrm{i}\mathcal{V})E,} \tag{16}$$

where $\mathcal{PS}_\mathrm{i}\mathcal{V}$ is the *incident transport operator*, a matrix that maps the emission function into a discretized incident global illumination solution. We understand the rotation to the local frame to be incorporated in $\mathcal{P}$. Since $\mathbb{X}_h$ is finite-dimensional, $\mathcal{P}$ is a measurement operator similar to $\mathcal{M}$: It consists of applying a set of dual basis functions to the solution, each of which corresponds to a single basis function of $\mathbb{X}_h$. (Note that this implies that techniques based on direct computation of adjoint solutions are applicable also in the factored context.) After the operator $\mathcal{PS}_\mathrm{i}\mathcal{V}$ turns the emission function E into a discretized incident illumination solution on the scene, the local operator $(\mathcal{MR})_x$ turns the incident solution into outgoing radiance at x. Figure 3 illustrates the steps. Since $\mathbb{X}_h$ is finite-dimensional and $\mathcal{M}$ produces a finite number of measurements, $(\mathcal{MR})_x$ is actually a finite matrix.[2] Furthermore, since by assumption the operator is only interested in the incident radiance at x, its discrete representation can be shared between many surface points. The simplest possible implementation of this scheme uses an albedo texture for describing the final reflection in a diffuse environment. The incident solution in $\mathbb{X}_h$ is a scalar function describing the incident irradiance, and applying $(\mathcal{MR})_x$ merely corresponds to multiplying the irradiance by the texture, turning it into outgoing radiosity. This is directly analogous to the radiosity technique of Gershbein et al. [1994].

Since the projector $\mathcal{P}$ works on incident, not outgoing, radiance, it is possible to define it in such a way that the incident global illumination solution is captured in free space around or inside the object in addition to surface points. The interpolated incident solution can be used for shading objects not originally present at precomputation time, although the global illumination solution will then not be exactly correct because it does not account for the presence of the new object. This is called "neighborhood transfer" by Sloan et al. [2002].

The choice of the spatial and directional bases and the associated projectors can be made in a number of ways. Most precomputed light transport techniques use an interpolatory projection in the spatial argument, that is, they point sample the transfer at the vertices and subsequently interpolate over triangles. This has the advantage that precomputation of the resulting compound operator $\mathcal{PS}_\mathrm{i}\mathcal{V}$ is easy:

[2]Some techniques that precompute subsurface scattering responses (cf. Section 3.1.4) implement the operator $\mathcal{MR}$ as a multiplication by a Fresnel term. The operator is then not strictly speaking a matrix, but still a linear operator.

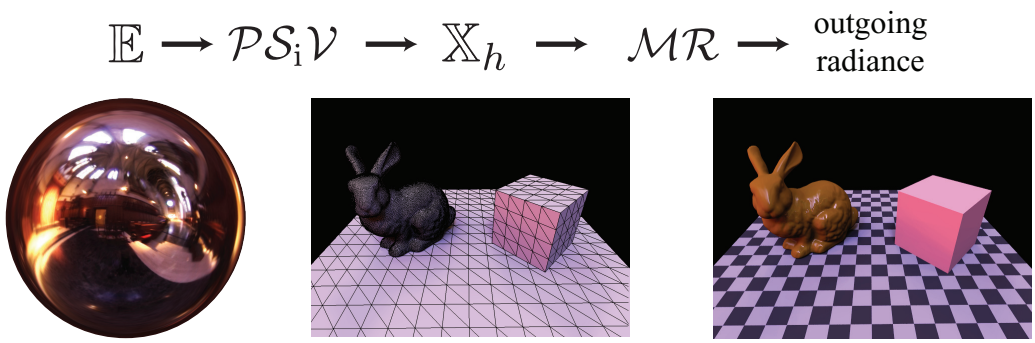

Fig. 3. Illustration of the factored version of the transport equation (16). The emission function (left) is mapped from the emission space $\mathbb{E}$ into to a discretized incident illumination solution in $\mathbb{X}_h(S \times \Omega)$ by the discretized solution operator $\mathcal{P}\mathcal{S}_{\mathrm{i}}\mathcal{V}$. The discretized solution (center) is represented in a tensor product of a spatial and a directional basis. Here the illustrated spatial basis is based on point sampling at the vertices, a usual choice in precomputed light transport algorithms. Here again irradiance is visualized, since the discrete incident solution is a 4D function. The spherical incident radiance function is interpolated from the spatial basis, and the final reflection is performed by the operator $\mathcal{M}\mathcal{R}$, which turns the incident solution into outgoing radiance (right).

One needs only to estimate a set of operators that map lighting from the emission space to a directional basis at each vertex and not worry about integrating over surfaces. In contrast, using an L_2 projection in the spatial argument requires additional surface integrals.

It is important to note that the result $\boldsymbol{r}_x$ is necessarily approximate, since information is lost in the intermediate projection to $\mathbb{X}_h$; that is, the projected incident solution does not agree with the real continuous solution exactly. This brings up the need to define the basis for $\mathbb{X}_h$ in a way that suits the final reflection operator. For instance, highly glossy final reflection will require substantial angular resolution in the incident solution. More precisely, the choice of the intermediate finite subspace $\mathbb{X}_h$ used for representing the discretized incident illumination solution is dictated by the reflective properties of the scene, and the kind of measurements contained in $\mathcal{M}$. For instance, in a purely diffuse scene the discretized incident solution can be represented using scalar irradiance functions—using a basis with directional variation would yield no benefit, since the outgoing radiance is view-independent also in the accurate solution. In a glossy scene the angular resolution of the functions in $\mathbb{X}_h$ should match the glossiness of the BRDF.

2.5 Finite Element Discretization of the Transport Operator Equation

Even in the case of a finite-dimensional $\mathbb{E}_h$, which we assume for the rest of this section, Equation (12) does not correspond directly to any finite element method. This is because the solution operator is included in its continuous form directly in the definition of the compound transport matrix, while a finite element method, on the other hand, works by constructing a discretized version of the transport operator $\mathcal{T}_{\mathrm{i}}$ and solves the associated discrete problem numerically. This necessitates the introduction of an intermediate discrete function space for approximating the incident illumination solution. This ties the finite element discretization closely to the factored transport Equation (16). Specifically, the finite element discretization of the incident illumination solution means constructing the abstract problem [Atkinson 1997]

$$\mathcal{P}\, L_{\mathrm{i}}^h = \mathcal{P}\mathcal{T}_{\mathrm{i}}\, L_{\mathrm{i}}^h + \mathcal{P}\mathcal{V}\, E \quad \Leftrightarrow \quad \mathcal{P}(\mathcal{I} - \mathcal{T}_{\mathrm{i}})\, L_{\mathrm{i}}^h = \mathcal{P}\mathcal{V}\, E. \quad (17)$$

Here $L_{\mathrm{i}}^h \in \mathbb{X}_h$ is the approximate incident illumination solution, and $\mathcal{P}$ is a projection operator that projects an incident radiance function into $\mathbb{X}_h$. Because the approximate solution is constrained to lie in $\mathbb{X}_h$ by the finite element assumption, Equation (17) is actually the linear system

$$\boldsymbol{l} = (\boldsymbol{I} - \boldsymbol{T}_{\mathrm{i}})^{-1}\, \boldsymbol{V}\boldsymbol{e}, \quad (18)$$

where the solution vector $\boldsymbol{l}$ contains the basis coefficients of L_{i}^h in terms of the basis of the approximating subspace, $\boldsymbol{e}$ is the basis coefficient vector that identifies E in terms of the basis of $\mathbb{E}_h$, $\boldsymbol{T}_{\mathrm{i}} = \mathcal{P}\mathcal{T}_{\mathrm{i}}$ is the discrete representation of the single-bounce transport operator, and $\boldsymbol{V} = \mathcal{P}\mathcal{V}$ is the discrete representation of the initial transport operator that has been constrained to $\mathbb{E}_h$. From the preceding it is clear that the product of the matrices in Equation (18) can be seen as the finite-element discretization of the incident transport operator $\mathcal{P}\mathcal{S}_{\mathrm{i}}\mathcal{V}$ from Equation (16). To obtain the final measurement vector, the approximate incident lighting solution must still be transformed by $\mathcal{M}\mathcal{R}$. Since L_{i}^h lies in a finite-dimensional space, $\mathcal{M}\mathcal{R}$ is actually a finite linear operator, as noted in the previous section.[3] Denoting $\mathcal{M}\mathcal{R} = \boldsymbol{M}$ to emphasize the finite size of the reflection and measurement operator, we get

$$\boldsymbol{r} = \boldsymbol{M}(\boldsymbol{I} - \boldsymbol{T}_{\mathrm{i}})^{-1}\, \boldsymbol{V}\, \boldsymbol{e}. \quad (19)$$

The product of the matrices in Equation (19) is the final finite element approximation to the compound transport operator $\mathcal{M}\mathcal{R}\mathcal{S}_{\mathrm{i}}\mathcal{V}$ from Equation (12).

The finite element solution $\boldsymbol{r}$ of Equation (19) is inherently less accurate than the one produced by the compound operator $\mathcal{M}\mathcal{R}\mathcal{S}_{\mathrm{i}}\mathcal{V}$ from (12). The accuracy of the finite element solution depends essentially on the capability of the approximating subspace $\mathbb{X}_h$ to represent the true lighting solution, and more importantly, its capability in representing effect of the continuous single-bounce transport operator [Arvo et al. 1994; Atkinson 1997]. In contrast, the "continuous" inversion by $\mathcal{S}_{\mathrm{i}}$ in Equation (12) guarantees, in principle, the optimal result. The difference is that in Equation (12) the exact solution is projected once in the end, while the finite element

[3]The reader may wish to derive formulae for the entries of $\boldsymbol{T}_{\mathrm{i}}$, $\boldsymbol{V}$ and $\boldsymbol{M}$. For this it suffices to substitute $L_{\mathrm{i}}^h = \sum_j l_j\, \psi_j$ and $E = \sum_k e_k\, C_k$ into Equation (17) and manipulate the resulting sums; here ψ_j and C_k are the basis functions of $\mathbb{X}_h$ and $\mathbb{E}_h$, respectively. The entries of $\boldsymbol{M}$ can be derived similarly by substituting the basis expansion for L_{i}^h into $\boldsymbol{r} = \mathcal{M}\mathcal{R}L_{\mathrm{i}}^h$ and remembering that $\mathcal{M}$ is actually a collection of separate measurement functionals.

solution involves an intermediate projection after each bounce of light. This can be best seen from the Neumann series for $(\boldsymbol{I} - \boldsymbol{T}_{\mathrm{i}})^{-1}$.

2.5.1 *Computing the Finite Element Transport Matrix.* In the context of a finite element method, solving for the discretized compound transport matrix from Equation (19) can be done using the Neumann series for $(\boldsymbol{I} - \boldsymbol{T}_{\mathrm{i}})^{-1}$. This results in the approximate solution matrix

$$\boldsymbol{M}(\boldsymbol{I} + \boldsymbol{T}_{\mathrm{i}} + \boldsymbol{T}_{\mathrm{i}}^2 + \ldots)\boldsymbol{V}. \tag{20}$$

Choosing to multiply the Neumann series by $\boldsymbol{V}$ from the right, this can be written in a recursive form as

$$\boldsymbol{M}\left[\sum_{j=1}^{\infty} \boldsymbol{L}_j\right], \quad \text{where} \quad \begin{cases} \boldsymbol{L}_0 = \boldsymbol{V} \\ \boldsymbol{L}_j = \boldsymbol{T}_{\mathrm{i}} \boldsymbol{L}_{j-1}. \end{cases} \tag{21}$$

Intuitively, this means taking $\boldsymbol{V}$, which is the matrix formed by basis expansions of the direct incident illumination on the scene due to all of the basis functions of $\mathbb{E}_h$, and reflecting them successively by applying $\boldsymbol{T}_{\mathrm{i}}$, always summing the result to a master copy. If only the intermediate incident lighting solution matrix from Equation (18) is desired, one simply skips the last multiplication by $\boldsymbol{M}$. The multiplication of $\boldsymbol{L}_{j-1}$ by $\boldsymbol{T}_{\mathrm{i}}$ can be thought of simply as a set of "gather" operations over the the whole scene. If the lighting solutions are diffuse, this procedure is equivalent to rendering a number of basis lighting solutions using a standard Jacobi iteration (gathering) variant of radiosity with the twist that the radiosity vectors denote incident irradiance, not outgoing radiosity. In a glossy setting this method parallels the nondiffuse global illumination method of Sillion et al. [1991], although there the authors stored outgoing radiance instead of incident radiance. Sloan et al. [2002] compute transport matrices exactly like this in their PRT technique. A similar algorithm is used also by Wang et al. [2006], with the difference that they store the radiance incident to scene points in a basis obtained from separable BRDF approximation, and that they truncate negligible values in the transport matrix after each step to conserve memory (many coefficients become small, since they utilize a wavelet basis on $\mathbb{E}_h$). Considering each column of the compound matrix separately, the above can also be viewed as a multiple right-hand-side linear problem, where the columns of $\boldsymbol{V}$ form the right-hand sides. This reveals that any other suitable iteration technique—for instance, "shooting" iteration [Cohen et al. 1988]—for solving linear systems of this kind is applicable.

Several previous finite element global illumination methods utilize hierarchical bases for the approximating subspace $\mathbb{X}_h$ [Hanrahan et al. 1991; Gortler et al. 1993; Sillion 1995; Christensen et al. 1996; Willmott et al. 1999]. To date, almost no precomputed light transport techniques have utilized comparable machinery for precomputation of the transport operators, with the exception of the direct-to-indirect transport methods of Kontkanen et al. [2006], Hašan et al. [2006], and Lehtinen et al. [2007]. The further adaptation of such methods for precomputed transport scenarios is a potential source of added efficiency in the precomputation phase (see Section 4.1).

2.6 Precomputed Light Transport Using Adjoints

This section discusses the adjoint formulation of precomputed transport. We observe that the computational efficiency of precomputed light transport is not really dependent on the low dimensionality of $\mathbb{E}_h$, but rather the efficiency of representing and applying linear functionals on $\mathbb{E}$—it just happens that a low-dimensional $\mathbb{E}_h$ always fulfills this condition.

Perhaps the simplest and most intuitive way of looking at the compound transport operator from Equation (12) is via the basis of $\mathbb{E}_h$. Each column of the operator is the measurement vector that corresponds to the global illumination solution computed using a single basis function of $\mathbb{E}_h$ as an emitter. This point of view leads one easily to conclude that in order for a precomputed light transport technique to be efficient, one must not use a basis with too many dimensions: One seemingly needs to compute an illumination solution and the corresponding measurement vector for each one of the basis functions. This can obviously require a significant amount of work. In addition, runtime evaluation of the novel lighting solution by multiplying the emission vector by the transport operator becomes more cumbersome as the dimension of $\mathbb{E}_h$ grows.

Looking back to Section 2.3, each measurement is associated with a corresponding adjoint solution defined on the emission space. The value of the measurement is computed as

$$r_i = \langle m_i, (\mathcal{R}\mathcal{S}_{\mathrm{i}}\mathcal{V})\, E\rangle_{\mathbb{X}} = \langle (\mathcal{R}\mathcal{S}_{\mathrm{i}}\mathcal{V})^*\, m_i, E\rangle_{\mathbb{E}} = \langle m_i^*, E\rangle_{\mathbb{E}},$$

where $m_i^* := (\mathcal{R}\mathcal{S}_{\mathrm{i}}\mathcal{V})^*\, m_i$ is the solution of the corresponding adjoint equation. In order to determine the value of the measurement for a given emission function, the inner product of the adjoint solution and the emission function must be computed. Now, if we restrict our attention to a low-dimensional $\mathbb{E}_h$, the computation of this inner product is always fast, for the simple reason that any m_i^* can be uniquely associated with a vector of length $\dim \mathbb{E}_h$ in a simple fashion, and hence the inner product reduces to that between two vectors of length $\dim \mathbb{E}_h$:

$$\langle m_i^*, E\rangle_{\mathbb{E}} = \left\langle m_i^*, \sum_{k=1}^{\dim \mathbb{E}_h} e_k\, C_k \right\rangle_{\mathbb{E}} = \sum_{k=1}^{\dim \mathbb{E}_h} e_k\, \langle m_i^*, C_k\rangle_{\mathbb{E}} = \boldsymbol{m}_i^T \boldsymbol{e}.$$

Here the C_k form the basis of $\mathbb{E}_h$, $\boldsymbol{e}$ is the coefficient vector that identifies E in terms of the basis, and the k:th component of $\boldsymbol{m}_i$ is $\langle m_i^*, C_k\rangle$. If $\mathbb{E}_h$ has low dimension, computing this inner product is obviously fast. Notice that we do not need to assume orthonormality of the lighting basis, and that the vectors $\boldsymbol{m}_i$ are exactly the *rows* of the compound transport operator when a fixed $\mathbb{E}_h$ is used.

An important observation from the above is that theoretically, for a given measurement m_i, the basis of $\mathbb{E}_h$ only comes into play after the corresponding (piecewise) continuous adjoint solution m_i^* on the full emission space $\mathbb{E}$ has been determined. Suppose now that we have a way of evaluating the exact adjoint solution. Then we are free to represent it in any way that we see fit, as long as our representation is such that it allows efficient computation of the inner product $\langle m_i^*, E\rangle$. Indeed, many relighting methods for real scenes estimate these adjoint solutions on the emission space by nonlinear approximation, for instance using Gaussian mixture models [Chuang et al. 2000]. In the synthetic context, an approach based on direct computation and nonlinear approximation of the adjoint solutions is taken by Green et al. [2006] in their precomputed transport technique. Comparable nonlinear approximation of the adjoint solutions, which are often called "reflectance functions," is also used in the reflectance field context by several authors, for example, Matusik et al. [2004], Peers and Dutré [2005], and Zongker et al. [1999]. See Section 3 for a more detailed discussion.

This observation can also be regarded as the basis for the efficiency of precomputed transport methods that use a wavelet basis on $\mathbb{E}$ [Ng et al. 2003; Wang et al. 2004, 2006]. These techniques may be seen as projecting adjoint solutions in the same orthonormal wavelet basis than the illumination. The solutions are, however, computed using the forward formulation; adjoint solutions then result from merely considering rows instead of columns. This results in vectors that correspond to the $\boldsymbol{m}_i$ in the preceding. These vectors are approximated nonlinearly by keeping only entries that have a nonnegligible magnitude, and consequently, computing the inner

product of the adjoint solution and the lighting vector only requires those entries of the vectors that are nonzero in both the lighting and the adjoint solution function. This effectively compresses the transport data.

Interestingly, it is apparent from the above deliberations that techniques based on approximating the adjoint solutions directly need not, in principle, even prescribe a basis for $\mathbb{E}_h$ a priori. (However, one must of course have a discrete representation of the adjoint solution in order to approximate it.) From a practical viewpoint, the ability to represent adjoint solutions on $\mathbb{E}$ in a compact form that allows fast integration with the emission function is sufficient for being able to compute the required illumination solutions.

3. CHARACTERIZATION OF PREVIOUS METHODS

This section presents an overview of methods that can be explained by our framework. After a brief introduction, we first present a simple taxonomy of such methods, and then proceed to give more detailed descriptions along with ties to the framework. Section 3.1 treats techniques for relighting synthetic scenes, while Section 3.2 discusses their counterparts for real scenes. We do not review all aspects of the presented techniques, since our goal is not to present comparisons between them in any other sense except showing how they connect to the present framework. Particularly, we treat techniques aimed at relighting real scenes more superficially than synthetic methods. We conclude with a concise review of methods for compressing the transport operators (Section 3.3).

A majority of the techniques reviewed in this section endow the emission space with a linear basis, and precompute or capture a global illumination solution for each of its degrees of freedom. Conversely, some techniques trace measurement functionals backwards to yield adjoint solutions on the emission space. This is the adjoint formulation of precomputed transport. Stacking all the illumination solutions together yields a finite representation of either the full transport operator $\mathcal{MRS}_{\mathrm{i}}\mathcal{V}$ from Equation (12) or the incident transport operator $\mathcal{PS}_{\mathrm{i}}\mathcal{V}$ from Equation (16). Obtaining the transport operators, be it by a forward or an adjoint method, is the goal of the precomputation or capturing stages of relighting techniques. Runtime relighting simply uses them for efficient computation of novel illumination solutions.

Methods that capture light transport from real scenes do not need explicit formulae for $\mathcal{V}$ or $\mathcal{M}$. Instead, they treat the scene as a black-box linear system and try to estimate the compound transport operator from the images taken under variable illumination. In practice this happens by lighting the scene by some known emission patterns, and recording a set of images of the scene under each one. Thus, the effect of the transport operator is produced implicitly. If the scene is lit by the basis functions of $\mathbb{E}_h$, these images directly form the columns of the transport operator, but many methods do not fix a basis beforehand and instead work by non linearly approximating adjoint solutions. Even though explicit formulae for the constituent operators that together form the compound light transport operator are of no significance to these methods, our framework still models the situation in a meaningful fashion.

Methods that can be explained by our framework can be characterized roughly by the following taxonomy. References and more exact descriptions are given further on. The borders between the categories are not always entirely clear—some techniques contain traits from more than one category.

Blending multiple lighting configurations (Section 3.1.1). Consider a static scene with multiple light sources, or groups of light sources. If a global illumination solution has been computed separately for each light source (group), turning lights on and off or changing their intensities is accomplished by weighting the different basis solutions appropriately.

Image and Texture Relighting (Sections 3.1.2 and 3.2.1). Image relighting is the fixed-view predecessor of precomputed transfer. An image of a scene is rendered under many basis illuminations, and the image that corresponds to a linear combination of basis illuminations is obtained by simply taking an appropriate linear combination of the basis images. A similar technique may be used for texture maps in order to capture local shadowing and interreflection effects. The techniques for real and synthetic scenes are analogous.

Precomputed radiance transfer (Sections 3.1.3 and 3.1.4). Precomputed transfer techniques render free-viewpoint images of synthetic scenes lit by distant environment maps, light sources with varying directional emission patterns, etc. Glossy reflections and subsurface scattering can be supported. The emission of light is usually described by a finite-dimensional emission subspace. Outgoing radiance is either captured directly in some directional function basis attached to each sample point in the scene, or through the factored transport Equation (16).

Environment matting (Section 3.2.2). Environment matting techniques extend traditional alpha matting by considering light transport from the backdrop onto the foreground objects. These are image relighting techniques with a very specific emission space.

Reflectance fields (Section 3.2.3). Reflectance fields represent the response of real scenes to lighting from different directions. The data is often captured either by fixing cameras around the scene and letting a light rotate around it, or by utilizing projectors. Some methods capitalize on symmetry of light transport. As these methods are image-based, all possible light transport mechanisms are captured automatically.

Bidirectional texture functions (BTFs) (Section 3.2.4). BTFs encode the spatially varying appearance of nearly flat real-world surfaces as a function of both incident lighting direction and the outgoing viewing direction. They are closely related to reflectance fields.

3.1 Synthetic Relighting

3.1.1 *Blending Between Lighting Configurations.* The simplest example of precomputed light transport is the case where illumination solutions that correspond to multiple physical lighting setups have been precomputed and are blended at runtime. Airey et al. [1990] present a radiosity-based method for interactive rendering of architectural walkthroughs where the user is able to control lighting interactively by linearly blending between radiosity solutions computed using different light source configurations. Here, the emission space is the linear span of the diffuse emission patterns of the light sources, that is, the DOFs control intensities of the individual light sources. This method fits in our framework simply by defining $\mathcal{M}$ as the collection of cosine kernels at surface patches that are used for computing radiosity. The initial transport operator $\mathcal{V}$ can be defined as in Section 2.2.

Dorsey et al. [1995] present a system for designing time-varying lighting for theatrical applications. Given sets of controllable stage lights and keyframes that specify their time-dependent intensities, the authors find an optimal basis for the vectors that describe the intensities by analyzing the keyframes by a singular value decomposition. Then, a global illumination solution is computed for each of these basis configurations, and the corresponding solutions are

blended at runtime to achieve the desired lighting sequence. Similar to the method of Airey et al., this method uses the emission functions of the groups of light sources as the emission space, but an additional basis change induced by the SVD is performed before rendering the basis solutions. The measurement operator $\mathcal{M}$ consists of pixel sampling filters, as the method relights images.

3.1.2 *Synthetic Image and Texture Relighting.* Image relighting methods aim to efficiently synthesize pictures of a static environment under time-varying lighting, viewed from a fixed viewpoint. Thus $\mathcal{M}$ consists of a set of pixel sampling filters in all of these techniques, while the emission space varies with each method.

The method of Nimeroff et al. [1994] produces pictures under different skylight scenarios. The authors introduce a steerable[4] spherical function basis and project the skylight into it. They then render basis images of the scene, each lit by a different lighting basis function. Relighting proceeds by simply weighting the basis images by the lighting vector. Teo et al. [1997] relight images in a similar fashion using a steerable function basis defined on the sphere of directions. Furthermore, they reduce the resulting set of basis images using PCA. These techniques use the span of steerable basis functions defined on the sphere of directions as the emission space; the operator $\mathcal{V}$ is simply the same as presented in the distant environmental illumination example in Section 2.2, and the measurements in $\mathcal{M}$ produce values for pixels. Wong et al. [2001] relight panoramic images, but do not consider indirect illumination. Their emission space is a set of directional lights, and the measurements produce pixel values for a panoramic image.

Dobashi et al. [1996] describe another method for relighting images under direct skylight. They essentially precompute the visibility to the sky for each pixel in the image (these are called "basis luminances" by the authors) expanded in a cosine basis, and use this information for relighting when the skylight or reflective properties of the materials change. The visibilities are compressed using vector quantization. The emission space is a special summed-area representation of the skylight.

Ng et al. [2003] describe an image relighting method for scenes lit by distant environmental illumination. The illumination function is represented by Haar wavelets defined over the faces of a cube map. The authors do note that there is nothing that would prevent the inclusion of also local, nondistant light sources in the lighting basis. Sharp shadows up to the limit prescribed by the resolution of the lighting environment are supported. Precomputation proceeds by rendering an image of the scene under each basis illumination by a ray tracer, or, if indirect lighting can be neglected, by rendering a visibility cube map as seen from each scene point hit by an eye ray. For a fixed image pixel i, the set of colors associated with each basis light comprises an adjoint solution m_i^*—see Equation (15)—defined on the cube map. This is called a "transfer function" by the authors. These solutions are transformed into the Haar basis and approximated by truncating negligible coefficients. Computing the value of a pixel under a novel illumination environment then boils down to a sparse vector dot product between the coefficients for the transfer function and the vector of coefficients that describe incident illumination in the Haar basis. The authors also note that in diffuse scenes this method may be used for relighting with changing viewpoints. In this case the irradiance cosine kernels replace the pixel sampling filters as the measurement functionals. The same wavelet cube map lighting representation is used by several other precomputed transfer techniques; see Section 3.1.3. Unfortunately, rotating the lighting function represented as wavelets is challenging, since the basis functions are not steerable, unlike for instance the spherical harmonics. Wang et al. [2006] treat the efficient rotation of similar wavelet expansions, but limit their attention to 2-DOF rotations.

Hašan et al. [2006] describe an image relighting technique capable of accounting for local (nondistant) light sources. They precompute a light transport operator that turns the irradiance incident to a scattered cloud of points in the scene into the image. After evaluating direct irradiance at these "gather points" using any suitable technique, the transport operator is hierarchically applied to yield an image with indirect illumination, including compelling glossy effects. In our terms, the emission space is defined by a set of point lights scattered on the surfaces on the scene, and the measurements are pixel sampling filters. Furthermore, as the precomputed operator only accounts for indirect illumination, the solution operator $\mathcal{S}_\mathrm{i}$ is formally modified by subtracting the identity.

Texture relighting techniques model the effect of variable illumination on patches of texture. When these patches are mapped onto objects in a scene, local self-shadowing and interreflection effects can be rendered at interactive rates. The appearance of the texture elements is view-independent, and thus these methods are justified only for diffuse surfaces or fixed viewing directions. Malzbender et al. [2001] light the texture by many directional lights, and fit the diffuse response of each texel to a biquadratic polynomial in the least-squares sense with respect to the incident lighting direction. This can be seen as approximating the adjoint solution for the texel by a polynomial. Malzbender et al. use their basis only for rendering with point-like light sources. Ashikhmin and Shirley [2002] propose a directional basis with the aim of being as tightly directional as reasonably possible while retaining approximate steerability. Their emission space is the linear span of these basis functions, and precomputation works by computing a separate solution for the texture under each basis light. Also the diffuse variant of the local precomputed transport method of Sloan et al. [2005] is essentially a texture relighting technique. However, they also treat view-dependent reflections (see Section 3.1.3).

3.1.3 *Precomputed Radiance Transfer.* Precomputed radiance transfer (PRT) has recently emerged as an active research topic. These methods relight synthetic, usually static scenes under dynamically varying illumination and changing viewpoints. Some methods work with diffuse reflectances, but many support glossy reflection, many provide full global illumination solutions, and some incorporate subsurface scattering. Most work has so far concentrated on distant environmental illumination.

Dobashi et al. [1995] render interactive walkthroughs of environments lit by static point lights with time-varying directional emission distributions. These distributions are modeled as linear combinations of the spherical harmonics. A radiosity solution is computed for each spherical harmonic basis function associated with each light source, and these radiosity solutions are then blended interactively in order to obtain the lighting solution that corresponds to the user-specified emission characteristics. The emission space $\mathbb{E}_h$ now has a DOF for each of the spherical harmonics used for defining the emission distribution of each of the light sources, and the measurement functionals are the cosine kernels over surface patches familiar from radiosity.

The kickoff for the active recent work on PRT was given by Sloan et al. [2002]. They assume the scene is lit by a distant lighting environment. The spherical incident radiance function is expressed as a low-order spherical harmonic expansion. In terms of our framework, this means that $\mathbb{E}_h$ consists of the linear span of

[4]A steerable function basis on the sphere is by definition closed under rotation.

the chosen number of spherical harmonics. Using only low-order basis functions implies that high frequencies in the incident lighting cannot be accounted for. Two methods, one for diffuse scenes and another for glossy scenes, are presented. The former corresponds to simply producing a radiosity solution sampled at scene vertices that corresponds to each spherical harmonic basis function on $\mathbb{E}_h$. Relighting proceeds by simply weighting these solutions by coefficients that describe the current lighting environment, exactly as suggested by Equation (14). In the context of our framework, this corresponds again to using cosine lobes centered on the surface normals at sampling points on the scene as the measurement functionals in $\mathcal{M}$. The glossy case may be seen in light of the factored transport Equation (16), where the intermediate space $\mathbb{X}_h$ is the tensor product of a set of spherical harmonics and linear "hat" functions centered at scene vertices. Projection into the spatial basis is performed simply by point sampling the transfer at the vertices. (This representation is used almost exclusively by precomputed transfer techniques.) The per-point incident transport matrices are evaluated by a technique that represents Jacobi radiosity that was described in Section 2.5.1. Final outgoing radiance, that is, the effect of $\mathcal{MR}$, is evaluated by spherical convolution implemented as multiplication in the spherical frequency domain. Because this requires a symmetric BRDF kernel, only Phong-like reflection functions can be supported. In follow-up work Kautz et al. [2002] present a BRDF integrator capable of arbitrary, also anisotropic BRDFs. However, the limitation of low-frequency incident lighting still applies. While Sloan et al. [2003] focus primarily on compression of the transport matrices, they also describe a renderer that accounts for subsurface scattering. Lehtinen and Kautz [2003] utilize a matrix representation for the BRDF in the same low-frequency context and project the outgoing radiance into a function basis with compact (small) supports. Křivánek et al. [2004] explore adaptive mesh subdivision during the precomputation of diffuse transport operators in order to focus computational efforts where they will make a visible difference. James and Fatahalian [2003] apply the diffuse version of the precomputed transfer method of Sloan et al. [2002] to models that can be deformed according to a precomputed simulation of dynamics. The diffuse transport operators are first computed for a sparse set of frames obtained in the simulation step. This large dataset is then compressed using global PCA. The transfer matrices are interpolated from the sparse samples for in-between frames by radial basis functions.

The biscale transfer technique of Sloan et al. [2003] is one of the motivators for the factored version (Equation (16)) of the present framework. The global incident transfer operator $\mathcal{PS}_\mathrm{i}\mathcal{V}$ is computed as described above, but the final surface interaction is implemented using bidirectional texture functions that have been transformed into the spherical harmonic basis in their light-dependent arguments. These transformed BTFs define the operators $(\mathcal{MR})_x$ from Equation (16). This allows the coarser global illumination solution to affect the minute details found in the BTF microstucture.

The Haar image relighting method of Ng et al. [2003] was extended to glossy objects and changing viewpoints in concurrent work by Liu et al. [2004] and Wang et al. [2004]. They make the observation that representing the BRDFs of surfaces by separable approximations [Kautz and McCool 1999] significantly reduces the number of basis functions required for representing outgoing radiance from surface points. These techniques can be seen as examples of the factored version of our framework, where the operator $\mathcal{PS}_\mathrm{i}\mathcal{V}$ measures the incident illumination solution by the incident factors of the BRDF approximation. The result produced by this operator is a coefficient vector that is used for modulating the outgoing factors of the BRDF approximation. The reflection and measurement operator $\mathcal{MR}$ can thus be seen merely as evaluation, modulation and summation of those outgoing basis functions. Wang et al. [2006] improve the technique by adding indirect lighting, and also describe a GPU-optimized renderer. Overbeck et al. [2006] analyze and exploit temporal coherence in similar all-frequency precomputed transfer techniques based on wavelets.

Tsai and Shih [2006] present a PRT technique for direct illumination where the distant incident illumination function is represented by scattered data approximation using spherical radial basis functions (SRBFs). The SRBF expansion for the incident illumination is found by nonlinear optimization. Transfer functions (i.e., adjoint solutions) that correspond to each vertex are represented in a linear basis built of SRBFs with fixed centers. Their technique also makes use of separable BRDF approximation. In terms of our framework, their technique projects the adjoint solutions to a fixed linear space, but does not fix a basis for $\mathbb{E}$ and relies instead on nonlinear approximation for the emission functions. Due to the radial symmetry of the SRBFs, computing the integrals $\langle m_i^*, E\rangle$, that is, the application of the adjoint solutions to the emission functions, can be performed efficiently.

Wang et al. [2005] treat relighting of plant models. They separate the distant incident illumination into three components: direct sunlight, indirect sunlight and low-frequency environmental illumination. The environmental component and indirect sunlight are rendered using the PRT technique of Sloan et al. [2002]. The direct sunlight component is captured using "light visibility maps," essentially precomputed shadow maps.

Sloan et al. [2005] present a local radiance transfer method that can be seen as a view-dependent extension to texture relighting. The method accounts for local view-dependent effects due to environmental lighting. Much like a BTF, the technique encodes a transport matrix for each texel in a texture that accounts for the local shadowing and interreflection effects caused by the patch of texture onto itself. In relation to our framework, the measurement functionals used by this technique are either irradiance cosines in the diffuse case, or the incident factors of a separable BRDF approximation in the glossy case. The main point is being able to cope with freely deforming objects by efficiently rotating the local transfer matrices from the current deformed orientation to match the incident lighting. The efficient rotation is achieved by nonlinearly approximating the adjoint solutions that correspond to each measurement by zonal harmonics.

Kristensen et al. [2005] describe a precomputed transfer method with the aim of relighting the scene with a dynamic, nondistant light in it. The emissions are parameterized by a set of fixed omnidirectional pointlights scattered in free space. Thus, the emission manifold is the continuous set of points in the volume, and $\mathbb{E}$ contains functions that describe isotropic volume emission at each point in the volume. The cloud of pointlights corresponds to a discretization of the continuous volume emission function by Dirac impulses; that is, $\mathbb{E}_h$ consists of the emissions of these pointlights. A global illumination solution is computed for each basis light, and relighting proceeds as usual by weighting and summing the basis solutions. The basis solutions are first computed to full resolution, and later compressed utilizing coherence both between scene points and the lights (see Section 3.3). Again, the measurement operator $\mathcal{M}$ may be seen as the irradiance cosine kernels at the vertices in the case of diffuse surfaces, while the appearance of glossy surfaces is approximated in the tensor product of a piecewise linear "hat" basis and the spherical harmonics. The authors note that best results are obtained when only the indirect component of the solution is precomputed and direct illumination is evaluated using traditional techniques.

Kontkanen et al. [2006] describe a finite element algorithm where the full solution operator of the discretized global illumination problem is represented hierarchically using wavelets. The operator maps direct illumination evaluated at the surfaces of the scene into indirect illumination, while direct illumination is rendered using traditional techniques. This enables the interactive rendering of indirect illumination due to arbitrary local light sources. The method has strong ties to previous hierarchical global illumination techniques [Gortler et al. 1993; Christensen et al. 1996]. The key difference is that the previous techniques use a hierarchical representation of the single-bounce transport operator in an iterative solution scheme with a known emission function, whereas Kontkanen et al. use similar mathematical machinery for precomputing the whole operator. This technique is a special case of our framework in that the emission space $\mathbb{E} = \mathbb{X}$, that is, the input to the operator is defined on the same space as the solution. This implies $\mathcal{V} = \mathcal{I}$. Note however, that the emission basis can still chosen to be different than the basis on $\mathbb{X}_h$. Furthermore, direct illumination is subtracted from the solution. In terms of our framework, this can be modeled by altering the solution operator $\mathcal{S}_\mathrm{i}$ by subtracting the identity. Lehtinen et al. [2007] describe a similar technique, but unlike Kontkanen et al. [2006], they do not utilize wavelets but define the hierarchical basis through a scattered data approximation procedure instead.

Green et al. [2006] describe a precomputed transport technique for distant illumination that is based on direct evaluation of the adjoint solutions that correspond to point measurements of the glossy component of the final reflection. The diffuse component is rendered using earlier methods. The authors solve the adjoint equations that correspond to the point measurements separately by tracing "importons" backwards in the scene. Once the particles land on the distant sphere, they are binned into the texels of a cube map. The result is an adjoint solution defined on $\mathbb{E}$. The distribution is then approximated nonlinearly by fitting a set of Gaussian functions. The Gaussians allow fast runtime integration of the adjoint solution against the incident lighting through the use of prefiltered environment maps. Since the adjoint solutions are computed directly, without fixing a basis for $\mathbb{E}$ a priori, all-frequency effects can be efficiently precomputed and represented.

There are several techniques that treat the efficient computation of the multiple product integrals that express direct, shadowed environmental illumination for glossy objects [Ng et al. 2004; Zhou et al. 2005; Sun and Mukherjee 2006]. They work by projecting the incident lighting, the visibility function, and the BRDF into a linear basis and exploring the properties of the integrals of the products of the expansions. While related to precomputed light transport, these techniques can only account for direct illumination. On the other hand, they are able to interactively change the BRDFs and even support dynamic scenes to an extent.

3.1.4 *Precomputed Subsurface Scattering.* Several techniques precompute or capture the subsurface scattering properties of translucent objects for relighting purposes. All these methods fall naturally within our framework. Most techniques only treat diffuse multiple scattering.

Hao et al. [2003] consider translucent meshes lit by directional lights. They compute the appearances of the mesh under a discrete set of distant lights by applying a BSSRDF to simulate subsurface scattering. This yields a set of scalars for each surface point and each lighting direction. Rendering proceeds by modulating these maps by a Fresnel term for the viewing direction. In follow-up work Hao and Varshney [2004] present a simple but reportedly effective predictive coding scheme for reducing memory requirements (see Section 3.3). These techniques may be seen in the light of the factored form of Equation (16), with the emission space being the set of directional lights, the intermediate transport and projection operator $\mathcal{P}\mathcal{S}_\mathrm{i}\mathcal{V}$ giving the incident subsurface irradiance from below the surface points, and the final reflection and measurement operator $(\mathcal{M}\mathcal{R})_x$ implemented by multiplying the subsurface irradiance by the Fresnel term for the outgoing direction. These methods do not account for indirect illumination. Sloan et al. [2003] include also view-independent subsurface scattering in addition to reflection in their precomputed transfer technique for distant low-frequency illumination. They also account for indirect illumination.

Lensch et al. [2003] describe a technique for relighting translucent meshes through precomputation of the object's response to incident local irradiance. The data is precomputed and stored in a two-level hierarchy. A coarse vertex-to-vertex transport matrix models large-scale, smooth subsurface transport. Small-scale local details are encoded in texture space using spatially-varying filter kernels. At runtime the two representations are blended together. The method of Goesele et al. [2004] utilizes the same two-component representation, but instead of synthesizing the impulse responses, they capture them from a real object. Carr et al. [2003] present a GPU implementation of a somewhat similar method. They work exclusively in texture space, and perform a multilevel decomposition of the transport matrix with respect to the senders, so that computing the product between the irradiance vector and the transport matrix is facilitated by a MIP-map pyramid of the incident irradiance function. These techniques can also be cast in the factored version of our framework by considering the emission space $\mathbb{E}$ to be the set of irradiance functions on the surface of the object, and, as in the above case of Hao et al., the transport and projection operator $\mathcal{P}\mathcal{S}_\mathrm{i}\mathcal{V}$ giving the incident subsurface irradiance at points on the mesh after self-shadowing and scattering according to the BSSRDF. The final reflection step again consists of merely the application of the Fresnel term. Since these techniques are based on the parameterization of the scattering response to irradiance on the surface of the object, they are nicely orthogonal to the lighting environment: They pose no requirements whatsoever as to how the initial surface irradiance that is subsequently fed to the transport matrix is obtained. For instance, local light sources can easily be supported. In this respect these techniques resemble the PRT method of Kontkanen et al. [2006].

Wang et al. [2005] describe relighting of translucent meshes using the BSSRDF approximation under distant illumination parameterized by Haar basis functions defined on a cube map. They precompute per-surface-point adjoint solutions that describe diffuse multiple scattering transport from the distant lighting environment, and approximate these adjoint solutions by by truncating near-zero Haar coefficients already during their computation. The authors also consider approximate single scattering in addition to diffuse multiple scattering. The view-dependence of single scattering is handled by employing an SVD-based separable approximation of the scattering phase function. For the diffuse part, the interpretation of this method in terms of our framework is the same as that of Hao et al. [2003], except for the compression of the adjoint solutions. The view-dependent part can be seen as a measurement of the direct, shadowed illumination by kernels that involve visibilities at surface points, incident Fresnel terms, the incident parts of the phase function approximation terms, and extinction factors.

3.2 Relighting Real Scenes

Debevec et al. [2000] define the *reflectance field* of a physical scene as the 8D function that relates unit incident lighting from any position and direction outside a closed surface S' enclosing the scene to the appearance of the scene as seen from any point outside the

surface. The surface S' may or may not coincide with the actual surface of the scene. When S' is contructed to follow the real geometry of the scene, the term *surface reflectance field* is used. In terms of our framework, the reflectance field clearly is before discretization the kernel of the solution operator $\mathcal{RS}_{\mathrm{i}}\mathcal{V}$, where the emission space $\mathbb{E}$ consists of functions on the 4D manifold $S' \times \Omega$; see Equation (11). Notice that in a fixed lighting condition this reduces to surface light fields, for example [Miller et al. 1998]. Fixing cameras to look at the scene corresponds to discretization by applying a measurement operator $\mathcal{M}$ that consists of pixel sampling filters. Discretization of the emission may be accomplished either simply by endowing a linear basis on $\mathbb{E}$, or by exploiting reciprocity and capturing adjoint solutions. Most relighting techniques based on this concept capture lower-dimensional *slices* of the reflectance field. For instance, assuming distant illumination reduces the dimensionality by two, and only capturing the appearance of the scene from one viewpoint also results in similar reduction, resulting in an image relighting method. Relighting real scenes by capturing images of the scene under different lighting conditions can be seen as real world parallels of precomputed transfer: What precomputed radiance transfer does on synthetic scenes, reflectance fields do on real objects.

Relighting techniques for real scenes usually parameterize the incident lighting (which is often but not always assumed to be distant) in some finite basis, although some techniques capitalize of symmetry and adjoints. One or more images of the scene are then recorded under each basis illumination. The appearance of the scene under a single basis light corresponds to a column of the transport matrix $\mathcal{MRS}_{\mathrm{i}}\mathcal{V}$, while each row corresponds to an adjoint solution associated with a single pixel. The scene may then be relit simply by weighing acquired images appropriately and summing them up. Data acquired in this fashion is often interpolated and extrapolated to give an approximation of appearance also to directions not originally covered by the cameras. Reflectance fields also capture nonlocal effects such as shadowing, interreflections and subsurface scattering because the outgoing light is captured from photographs, so that light has actually reached the point in question through a number of different paths, only one of them being direct. Because these techniques work by actually pointing lights at the scene, the action of the operator $\mathcal{V}$ is defined implicitly.

3.2.1 *Image and Texture Relighting in Real Scenes.* As stated above, methods that relight images of real scenes capture a subset of the full reflectance field that corresponds to the set of rays defined by a camera in fixed position. Masselus et al. [2003] relight images of scenes under a 4D incident lighting basis to account for local (nondistant) illumination effects. Nayar et al. [2004] describe a display that relights a static image according to the lighting conditions in which the display is viewed in, under the assumption of distant illumination. The system presented by Wenger et al. [2005] captures a relightable image sequence of an actor's performance in real time.

Hawkins et al. [2005] exploit reciprocity in their image relighting technique for distant illumination. They place the subject inside a hollow sphere with diffuse inner walls and fix a fisheye camera looking at the inside of the sphere. A laser ray is then shot through each pixel in the image towards the subject, and the pattern of light that is produced on the inside walls of the sphere after interaction with the subject is recorded by the camera through a fisheye lens. Due to symmetry, this distribution corresponds to the whole spherical adjoint solution associated with the single pixel in the image to be relit. Integrating it against a novel spherical emission function gives the intensity of the pixel. This method has a notable similarity to the precomputed transfer technique of Green et al. [2006], who explicitly compute the spherical adjoint solutions that correspond to point measurements of the outgoing radiance function, also assuming distant incident illumination.

3.2.2 *Environment Matting.* The aim of alpha matting is to replace the background of an image with a new one, blue screening being a classic example. Environment matting techniques extend alpha matting by considering light transport from the backdrop to the foreground. This allows, for instance, specular objects to reflect the backdrop in the final image. In terms of our framework, this corresponds to defining $\mathbb{E}$ on a virtual rectangle behind the scene as seen by a camera, and measuring the lighting solution by pixel sampling filters. Techniques that capture environment mattes use a monitor placed behind the subject for emitting illumination.

Some techniques work in a "forward" fashion by defining a basis on $\mathbb{E}_h$ and rendering or capturing basis solutions for each element of the basis. Peers and Dutré [2003] utilize Haar functions, but capture only solutions for those basis functions considered important by an oracle that works through feedback from previously captured basis images. This corresponds to directly capturing columns of the transport operator. Other techniques work through adjoints by estimating the adjoint solution for each pixel directly through nonlinear optimization. These adjoint solutions are called *reflectance functions* in much of the environment matting literature, and they correspond exactly to the m_i^* from Equation (15), where the original measurement functionals m_i are pixel sampling filters. Zongker et al. [1999] approximate the adjoint solution by a single axis-aligned box on the backdrop, while Chuang et al. [2000] upgrade the representation to a Gaussian mixture model. Peers and Dutré [2005] employ wavelet noise patterns on the backdrop for estimating the per-pixel adjoint solutions represented sparsely in the Haar basis. Matusik et al. [2002] combine environment matting with distant directional illumination to yield two-component reflectance fields that allow rendering of transparent and refractive objects in novel, global lighting environments.

3.2.3 *Higher-Dimensional Variants.* Wong et al. [1997] describe a relightable Lumigraph [Gortler et al. 1996]. The incident illumination is assumed to be distant. The apparent intensities of points on a geometric proxy (a portion of a plane) are sampled as a function of incident lighting direction for a single viewing direction. The light dependence is represented as a spherical harmonic expansion at each point. The same procedure is repeated separately for a number of viewing directions. In terms of our framework, this can be seen (similar to the polynomial texture map technique of Malzbender et al. [2001]) as spherical harmonic approximation of the spherical adjoint solutions that correspond to point measurements of the outgoing radiance.

Surface reflectance fields [Debevec et al. 2000; Koudelka et al. 2001; Hawkins et al. 2004] can be captured by taking multiple images of the subject under each basis light. The emission space $\mathbb{E}_h$ is usually defined by distant directional lights in some fixed set of directions. The acquired images are projected on the surface of a geometric proxy such as the visual hull. These techniques often treat adjoint solutions explicitly. In the case of a global, fixed lighting basis, this merely amounts to considering rows instead of columns in the transport operator. Weyrich et al. [2005] describe a method for rendering deformed surface reflectance fields. Matusik et al. [2002] encode a surface reflectance field on the visual hull of the object, along with a view-dependent opacity function. This allows relighting of extremely complex objects, for instance furry animals or trees. Goesele et al. [2004] capture the diffuse subsurface response of an object to surface irradiance, and represent it the two-component

form described by Lensch et al. [2003]. While not exactly a surface reflectance field in the usual sense, their data is a spatially varying four-dimensional appearance model of a real object.

The symmetry of light transport allows exchanging the roles of the lights and the cameras while capturing the reflectance field. This enables the capture of reflectance fields with a higher-fidelity emission space in less time [Sen et al. 2005], since many cameras can observe the subject simultaneously without interfering with each other. Garg et al. [2006] capture a subset of the full 8D reflectance field using a hierarchical algorithm based on representing blocks within the light transport matrix by rank-1 approximations. The algorithm proceeds coarse to fine, stopping refinement whenever the rank-1 approximation is deemed sufficient. Due to their symmetric camera/projector setup, they can measure the rank-1 blocks directly by illuminating the scene by only two patterns.

3.2.4 *Bidirectional Texture Functions.* Bidirectional texture functions or BTFs [Dana et al. 1999] are 6D functions of position, lighting direction, and viewing direction, where each entry determines the view-dependent appearance of a single point as a function of distant lighting direction. The spatial parameter is assumed to lie on a patch that is flat on large scale. Thus BTFs may be seen as view-and-light-dependent texture maps that can be pasted onto new geometries similar to usual albedo textures. BTFs can be seen as reflectance fields where the incident illumination is assumed to be distant. In relation to our framework, the BTF can be thought of comprising a set of per-point transport matrices $\mathcal{M}_x\mathcal{R}\mathcal{S}_\mathrm{i}\mathcal{V}$, where the emission space $\mathbb{E}_h$ is a discrete set of directional lights, and the measurement operator $\mathcal{M}_x$ produces a set of area-averaged measurements of the outgoing radiance into a fixed set of directions. These matrices are often called apparent BRDFs.

3.3 Compression

Even after constraining the space of possible emissions, discretized light transport operators consume a significant amount of memory. Basically, the size of the raw matrix grows with the dimension of the measurement vector and the dimension of basis used for representing incident illumination; that is, the transport operator has dimension $m \times \dim \mathbb{E}_h$, where m is either the dimension of the measurement vector, or the dimension of the basis of the space $\mathbb{X}_h$ used for representing the incident illumination solution if the factored representation from Equation (16) is used. Furthermore, even if the emission basis is relatively low-dimensional, computing the outgoing radiance is a heavy procedure, particularly when view-dependent glossy reflections are desired. Compression techniques for precomputed light transport operators aim not only to reduce the size of the precomputed operator, but also facilitate its fast application at runtime. This dual goal is different from most compression algorithms, which usually aim only at data reduction. In the following we review techniques for compressing light transport operators, but do not touch rendering performance issues.

The large size of the matrix has been mainly dealt with in three ways: One can either settle for a low-dimensional $\mathbb{E}_h$, rely on nonlinear approximation of the adjoint solutions that correspond to each measurement, or compute all the data first and then run it through a compression algorithm. A fourth alternative, only representing the transport operator to within required precision already by design of the precomputation algorithm, has so far received limited attention. We present some ideas on this alternative in the synthetic context in Section 4.

In most realistic uses, just settling for a low-dimensional $\mathbb{E}_h$ will not suffice. Consider the precomputed transfer method of Sloan et al. [2002] that uses a 25-term spherical harmonic basis for representing incident illumination. Even in the case of a diffuse receiving surface, where the per-point transport operators $\mathcal{M}_x\mathcal{R}\mathcal{S}_\mathrm{i}\mathcal{V}$ only have one row, this amounts to 25 numbers per color channel per vertex. Already this amount of data can be prohibitively high given the geometric complexity of modern scenes. The situation quickly gets worse if glossy reflections are required, as this requires adding rows to the transport operator. It is possible to combat this by using a separable approximation for the BRDF, as the number of significant outgoing basis functions resulting from the SVD approximation is low for many BRDFs, but this alone does not suffice to bring storage requirements to a tolerable level.

In their image relighting system, Teo et al. [1997] perform principal component analysis (PCA) on the basis images obtained for each basis function on $\mathbb{E}_h$. They report modest savings in data size. In a similar vein, Koudelka et al. [2003] apply PCA over apparent BRDFs in order to compress bidirectional texture functions. An analogous technique is described in the low-frequency precomputed radiance transfer context by Lehtinen and Kautz [2003]. These techniques are global in the sense that the PCA is applied to the whole set of basis images or solutions. This undermines the efficiency of the resulting global linear model, because the inherent geometry of the space of transfer matrices is not low-dimensional when considered for the whole scene. However, when constrained to a small spatial neighborhood, light transport *is* low-dimensional in many cases. This observation, which is analyzed mathematically by Mahajan et al. [2007], is the basis for clustered (local) principal component (CPCA) approaches. The CPCA approach was introduced to compressing light transport operators by Sloan et al. [2003], whose technique iteratively finds clusters of spatial samples whose transfer matrices can be described well in a locally low-dimensional basis. The CPCA technique has found use in many subsequent algorithms. It has also been applied to compression of BTFs [Müller et al. 2003]. A global trilinear (space $\times$ view $\times$ light) approach based on a multimode SVD has been proposed for the compression of BTFs [Vasilescu and Terzopoulos 2004]. Despite its global nature, the technique performs better than global PCA. See the survey by Müller et al. [2005] for an in-depth discussion of BTF compression. A trilinear factorization approach is combined with local clustering in the synthetic precomputed transport scenario by Tsai and Shih [2006].

An approach based on clustered PCA is described also by Matusik et al. [2002] as a part of their scheme for compressing reflectance fields. Their data is a set of pictures of the subject for each incident lighting direction. The authors compress the data in image space separately for each view by applying PCA with respect to the lighting direction in 8×8 pixel blocks—the difference from the CPCA of Sloan et al. [2003] is that Matusik et al.do not learn the clusters but fix them in advance. In all, the size of the resulting data is an order of magnitude less than the original. The greater efficiency stems from the local neighborhood in which the PCA is applied. In a similar vein, Nayar et al. [2004] compress pixel blocks in their relighting system, and extend the technique for exploiting spatial coherence in the lighting-dependent per-block PCA factors over the whole image. Garg et al. [2006] approximate blocks within the reflectance field matrix by rank-1 outer products.

Nonlinear wavelet approximation of the adjoint solutions associated with each point and each outgoing basis function is another major category of methods for compressing transport operators [Ng et al. 2003; Liu et al. 2004; Wang et al. 2004, 2006; Cheslack-Postava et al. 2007]. Most of these techniques compress the matrices of all surface points separately by truncating the wavelet coefficients of the adjoint solutions, that is, the rows of the transfer matrices. Cheslack-Postava et al. [2007] explore the use of higher-order

wavelets for the rows in an image relighting context, and also compress the columns of the matrix using wavelets from the image compression literature. Their technique is thus a true 4D compression algorithm that also adapts to spatial coherence in the image.

Green et al. [2006] approximate the adjoint solutions that correspond to point measurements of the glossy component of the final surface interaction by a Gaussian mixture model whose parameters are found by nonlinear optimization. This results in a compact representation for all-frequency effects.

Hao and Varshney [2004] describe a predictive coding scheme for transfer vectors that describe diffuse subsurface scattering. They select a small number of reference points on the mesh and store their associated transport vectors in full detail. For nonreference points, the differences of their transport vectors and those obtained by interpolation from the nearest reference points are encoded in low-order spherical harmonics. The authors report a reduction of about an order of magnitude in storage requirements.

Kristensen et al. [2005] describe a compression scheme for precomputed light transport operators that simultaneously adapts to coherence in both the spatial domain and with respect to the lighting responses. The surfaces on which transfer matrices have been computed are first split into disjoint clusters. Then, for each of the surface clusters, the lighting basis (which is a set of omnidirectional pointlights in the scene) is clustered separately by recursively merging together the lights whose responses (the columns of the transfer matrices) are the most similar over sample points in the current cluster. This step reduces the light basis in a way that best suits the surface cluster in average. Finally, the reduced set of transfer matrices is compressed using clustered principal components, that is, the sample points in the cluster are partitioned into even smaller subclusters, over which the matrices are modeled by linear combinations of basis matrices obtained by PCA. As the local PCA treats all entries of the matrices equally—they are flattened to long vectors before applying the SVD—the basis matrices found by PCA approximate the general linear trend in the matrix data, that is, they model overall variation across all views and all lights simultaneously.

A common trend in almost all precomputed or captured light transport techniques is that they precompute the data first to full precision and subsequently compress the data. At least from an idealistic point of view, the expensive computation of data that will be thrown away by compression should ideally not happen at all. Some recent techniques take measures in order to limit the computation already during precomputation or acquisition. On the synthetic side, these include the hierarchical direct-to-indirect precomputed transport techniques of Kontkanen et al. [2006] and Lehtinen et al. [2007], and the image relighting algorithm of Hašan et al. [2006]. On the side of techniques that capture light transport in real scenes, the environment matting methods of [Peers and Dutré 2003, 2005], and the reflectance field systems of Matusik et al. [2004], Garg et al. [2006] and Sen et al. [2005] try to only compute the transport operators to some finite precision in the first place.

4. PERSPECTIVES ON NEW METHODS

The aim of precomputed light transport techniques is to compute and store the linear operators that map emission functions from the emission space onto global illumination solutions represented usually as either images or basis expansions. In other words, the result is a finite representation of the large linear operator that describes the transport. This operator may be represented either as a set of basis lighting solutions that correspond to fixed basis functions on $\mathbb{E}_h$, or adjoint solutions that correspond to individual measurements made of the solution. This section discusses some thoughts on future research directions in precomputed light transport. In particular, faster precomputation algorithms could be developed based on previous hierarhical and otherwise adaptive rendering algorithms.

4.1 Operator Approximation by Hierarchical Finite Element Methods

As was seen in Section 3, many precomputed light transport algorithms work by endowing the emission space with a hierarchical basis composed of wavelets. This easily allows the nonlinear approximation of the adjoint solutions that correspond to single measurements of the resulting illumination solution by truncating small-magnitude wavelet coefficients. However, most present algorithms precompute these adjoint solutions separately for each measurement (image pixel or spatial basis function) in a brute-force manner. For a high-fidelity emission space, this often results in precomputation times of hours or even days, which is clearly a limiting factor considering the practical use of these techniques. The precomputed data is subsequently run through a compression algorithm that aims to reduce storage by exploiting coherence in the transport between the measurements, i.e., scene points or image pixels. As all the data is computed first and compression performed afterwards, this is a bottom-up procedure. In contrast, a fully hierarchical precomputation technique would utilize coherence between scene points, viewing directions and lighting basis functions already during precomputation—computing everything and compressing later is, at least from an idealistic point of view, clearly a waste of resources.

On the other hand, previous hierarchical finite element methods such as hierarchical radiosity and its extensions (e.g., [Hanrahan et al. 1991; Gortler et al. 1993; Smits et al. 1994; Sillion 1995]) and the glossy wavelet methods of Christensen et al. [1996, 1997] compute illumination solutions by representing the single-bounce light transport operator as a collection of *transport links* between hierarchical basis functions,[5] and refining these interactions between parts of the scene in a top-down manner only to the level deemed necessary by an oracle function. In the context of wavelets, this means that many entries of the transport matrix will be close to zero. *The aim of hierarchical top-down refinement is not to compute insignificant entries of the transport matrix in the first place.* The solution of the global illumination problem proceeds by iterating between solving for the equilibrium lighting solution described by the current approximation of the transport operator, and refining the hierarchical representation of the operator according to where significant energy transfers were made.

Recently, Kontkanen et al. [2006] presented a precomputed transport algorithm that extends this hierarchical machinery for actually computing a hierarchical representation of the solution operator of the illumination problem. Specifically, they precompute an operator that maps a direct lighting function, represented as a Haar expansion on the surfaces of the scene, into another Haar expansion that describes indirect illumination. Once the direct illumination has been computed per-frame using traditional techniques, application of the precomputed operator produces indirect illumination. This direct-to-indirect operator is precomputed by evaluating the Neumann series using a wavelet discretization of the single-bounce operator familiar from the earlier hierarchical algorithms. The series

[5]The term "basis function" should be understood loosely. For instance, clusters of objects and volume emitters can be used as the entities between which light transport takes place. That is, one need not be constrained to function hierarchies e.g., within a single polygon.

is computed by repeatedly multiplying the wavelet representation of the single-bounce transport operator by itself and summing the powers together. This matrix-matrix multiplication is fast, since the operator is sparse. The technique handles, in principle, glossy transport in addition to diffuse. The discretized solution operator may be viewed as a wavelet discretization of the global reflectance distribution function (GRDF) [Lafortune and Willems 1994], which is the kernel function of the solution operator $\mathcal{S}_\mathrm{i}$.

The technique of Kontkanen et al. [2006] can be seen as a special case of a general, as yet largely unexplored, pattern of hierarchical precomputation algorithms based on previous hierarchical finite element and related methods. Such techniques exploit both spatial and light coherence simultaneously. An algorithm for distant illumination could be constructed by utilizing hierarchical bases both on the emission space and for representing the spatial and possibly angular variation in lighting functions on the scene. The choice of basis is discussed in the following. The solution would proceed by first producing a finite hierarchical discrete representation of $\mathcal{V}$. The entries of this discretized operator are transport links from emitter basis functions onto receiving basis functions on the scene. They are analogous to the links utilized by the previous hierarchical algorithms, and also analogously, will exhibit sparsity owing to the nature of hierarchical bases. Once this operator has been computed, it would be repeatedly multiplied by a hierarchical representation of the same one-bounce discretized transport matrix as utilized by Kontkanen et al., according to Equation (21). The end result is a discrete representation of $\mathcal{S}_\mathrm{i}\mathcal{V}$, which may then be complemented with a suitable final reflection and projection operator $\mathcal{MR}$. The key difference to earlier progressive solvers [Sloan et al. 2002; Wang et al. 2006] is that the computation of the bounces utilizes a hierarchical transport operator, in effect sharing work between multiple surface samples.

Since the emission function is unknown at precomputation time, the bound on the energy transfer through a link in the hierarchical one-bounce transport operator cannot be used for guiding refinement of the operator representation (this is the "BF refinement" scheme proposed by Hanrahan et al. [1991]). However, if the measurements in $\mathcal{M}$ were to be brought into play from the beginning, an adjoint or bidirectional method that uses a hierarchical representation for measurement functionals could bound discretization error by the "potential" transported by the link to the opposite direction. Analogous to the bidirectional radiosity technique of Dutré et al. [1996], this would in a way correspond to multiplying the Neumann series in Equation (20) by $\boldsymbol{M}$ and $\boldsymbol{V}$ simultaneously instead of just multiplying by $\boldsymbol{V}$ from the right.

Kontkanen et al. [2006] base their technique on Haar wavelets and a so-called standard decomposition [Beylkin et al. 1991] of the transport operator $\mathcal{T}_\mathrm{i}$. It should be straightforward to extend their technique to higher-order (multi-)wavelet bases utilized in prior wavelet radiosity algorithms [Gortler et al. 1993]. Unfortunately, such approaches will suffer from problems carried over from these earlier algorithms. These include the well-known difficulty of chartifying and parameterizing the input surfaces, and the inevitable visible discontinuities between charts. Indeed, the technique of Kontkanen et al. is demonstrated only on scenes consisting of uniformly sized quads. Even though there is recent work on extending wavelet radiosity to more difficult meshes [Lecot et al. 2005], visible discontinuities between charts still remain. Utilizing discretizations based on clusters of input primitives, as employed by face cluster radiosity [Willmott et al. 1999], its higher-order variants [Gobbetti et al. 2003], and volume clustering techniques [Sillion 1995] has seemingly not been explored in the PRT context. Techniques based on volume clustering should be able to adapt to highly difficult geometry such as dense foliage, although discontinuities between clusters will still be apparent. Meshless (hierarchical) function approximation techniques (see Section 4.4) offer interesting alternatives that do not suffer from cluster or chart boundaries. However, if only indirect illumination is represented in the basis and direct lighting is rendered using traditional techniques, the discontinuity problems will not be as acute.

A potential mathematical complication in cluster-based finite element algorithms is that in their current form they rely on the nonstandard operator decomposition [Beylkin et al. 1991]. This means that the solution is represented in an overcomplete multiresolution expansion, much like a mip-map pyramid. While it is algebraically possible,[6] computing powers of the nonstandard discrete operator representation seems significantly more complicated than in the case of a standard decomposition. However, it seems straightforward to define a difference-based function space on such clusters, which would allow the use of a standard decomposition.

4.2 Path Tracing with Hierarchical Bases

It should also be possible to combine hierarchical function spaces on both the emission space and the scene with path tracing algorithms. We illustrate the idea on a diffuse scene for simplicity and assume orthonormal bases. The result would be an adaptive precomputation algorithm that proceeds coarse-to-fine both on the emission space and the spatial functions. A simple algorithm would generate paths starting only from the coarse receiving basis functions on the scene. After sampling a point on the support of a receiving function, a path would be generated from it similarly to eye ray tracing. At each intersection with the scene, a random point on a coarse emitter basis function would be sampled, and its contribution to the end of the path on the scene would be computed according to $\mathcal{V}$. This way, the multidimensional integral that determines the effect of the emitter function onto the spatial function can be estimated. It should also be possible to construct a bidirectional algorithm that also generates paths starting from the emitter samples.

Hierarchical refinement should be driven by measuring the smoothness in the kernel function of $\mathcal{RS}_\mathrm{i}\mathcal{V}$; clearly, in parts of the domain where the kernel is smooth, light transport does not need to be resolved to a high resolution, and conversely fast variation in the kernel is a sign of light transport features that need to be resolved more accurately. This corresponds to the task of the so-called *oracle* functions in hierarchical finite element global illumination methods. Because the kernel includes indirect illumination as well, measuring its smoothness directly seems difficult. A simple approximation would be for instance to monitor the throughputs of the direct paths from the emission basis to the spatial basis, in effect driving the subdivision according to direct shadows.

A similar approach could be formulated also for image relighting using a hierarchical emission basis [Ng et al. 2003]. The image would be divided into blocks, each of which would be fit with either a wavelet or comparable basis. Then, a path tracing algorithm similar to the one described above would monitor the variation across the image block and the emitter basis functions, and recurse deeper into the hierarchy according to an oracle. It is intuitively clear that homogenous image blocks will not require many basis functions for representing the spatial variation. Furthermore, the coefficients for basis functions in smooth regions could likely be computed using significantly fewer total samples than a brute-force per-pixel algorithm would use. This process can be roughly thought of as

[6] This can be seen by using the "telescoping sum" version of the nonstandard decomposition, see Equation 2.24 in the paper by Beylkin et al. [1991].

adaptive supersampling of the image with respect to both the lighting basis functions and image location.

4.3 Metropolis Light Transport

Green et al. [2006] describe a PRT technique based on nonlinear Gaussian approximation of adjoint solutions that correspond to point measurements of the outgoing illumination. These solutions are computed using reverse photon mapping. Once the photons land on the environment sphere after interacting with the scene, they are binned into texels of a cube map, which is subsequently used for fitting the Gaussians. The technique can thus be viewed as an adjoint algorithm based on particle tracing. The procedure is heavy, since it is performed separetely for spatial sample point and view direction.

Metropolis sampling was introduced for solving light transport problems by Veach and Guibas [1997]. The algorithms produces random points on the image plane that are distributed proportionally to image brightness. Conceptually, the Metropolis light transport algorithm could be extended for computing distributions that are proportional to the kernel of $\mathcal{R}\mathcal{S}_{\mathrm{i}}\mathcal{V}$ instead of image brightness. The result would then be a higher-dimensional distribution over both the scene points, viewing directions, and the emission space. (The situation is easier to visualize in 2D diffuse flatland.) This would result in sharing of work between many scene points and view directions compared to the brute-force algorithm. The resulting distribution would then be approximated in a suitable way, perhaps again through fitting Gaussians or in a linear hierarchical basis, in order to get a compact representation for the transport operator.

4.4 Meshless Techniques

Although it seems feasible to utilize both wavelets and cluster-based function spaces for discretizing the spatial variation in precomputed light transport operators, visible cluster or chart boundaries remain a noticeable visual problem. This suggests searching for alternative ways for sparsely representing lighting functions on the scene. Several rendering techniques based on scattered data approximation and interpolation offer promising leads.

Previous techniques for adaptive sampling and interpolation of irradiance [Ward et al. 1988] and radiance [Křivánek et al. 2005] functions, respectively, should be easily adaptable for the spatial discretization of the precomputed transport operator. More precisely, the spatial basis of $\mathbb{X}_h$ (see Sections 2.4 and 2.5) would consist of basis functions induced by the approximation procedure, while the projection coefficients are obtained through point sampling at the nodes. This would simply mean adaptively sampling light transport matrices in the spatial domain and extending the samples to the whole domain by the scattered approximation procedure. Note that the adaptive meshing technique proposed by Křivánek et al. [2004] has the same goal, but relies on the mesh for interpolation. Lehtinen et al. [2007] introduce a hierarhical scattered data approximation procedure for representing lighting functions and describe how such function spaces fit in a finite element context analogous to wavelets. This enables the formulation of meshless alternatives for many previous finite element techniques, including a large portion of the previous precomputed light transport methods. The hierarchical formulation results in sparseness of operator discretizations, which cannot be obtained through the previously mentioned non-hierarchical scattered approximation schemes.

The main advantages of meshless techniques are the lack of charts or clusters of input polygons and the resulting smooth and visually pleasing reconstructions of lighting functions, and the decoupling of the geometric representation of the scene from the function spaces used for describing the light transport. Indeed, such a decoupling has proved immensely successful in the off-line rendering context [Ward et al. 1988; Wann Jensen 1996]. Combining such a spatial sampling strategy with separable BRDF approximation should yield a compact representation for glossy transport. Also, combinations with biscale techniques for the final reflection would be straightforward. Note that these spatial scattered data approximation and interpolation techniques differ from the spherical approximation described by Tsai and Shih [2006]—they sample the spatial variation traditionally in the vertices.

5. CONCLUSIONS

We have presented a mathematical framework that can be used for classifying a large number methods that either precompute or measure the light transport in a scene. The framework is given in the form of an operator equation, where an emission function from an emission space $\mathbb{E}$ is mapped into a set of linear measurements of the resulting global illumination solution. The transport operator can be seen as consisting of either illumination solutions that correspond to each basis function of a finite subspace $\mathbb{E}_h$, or as a set of adjoint solutions that each produce the value of a single linear measurement of the global lighting solution when integrated against the emission function. As the equation is an extension of the well-known rendering equation, many previous global illumination techniques can be easily adapted for its solution. We have pointed out the conceptual similarities between many particular techniques by considering them as special cases of the framework. On a practical level, the framework should facilitate the transfer of ideas from one application area to another, and on a more abstract level, hopefully provide an unifying view for aiding future research.

ACKNOWLEDGMENTS

The author sincerely thanks Timo Aila for guidance and discussions; Jan Kautz, Janne Kontkanen and Samuli Laine for comments on the manuscript and discussions; Lauri Savioja for support; Frédo Durand and Paul Green for discussions; Per Christensen for input on inner products; Wojciech Matusik for the measured BRDF used on the bunny [Matusik et al. 2003]; Paul Debevec for the Grace Cathedral lighting environment (`www.debevec.org/Probes`); the Stanford Computer Graphics Laboratory for the bunny model; the anonymous reviewers for comments and constructive criticism.

REFERENCES

AIREY, J. M., ROHLF, J. H., AND BROOKS, JR., F. P. 1990. Towards image realism with interactive update rates in complex virtual building environments. In *Proceedings of the Symposium on Interactive 3D Graphics*. ACM Press, 41–50.

ARVO, J., TORRANCE, K., AND SMITS, B. 1994. A framework for the analysis of error in global illumination algorithms. In *Proceedings of ACM SIGGRAPH*. ACM Press, 75–84.

ASHIKHMIN, M. AND SHIRLEY, P. 2002. Steerable illumination textures. *ACM Trans. Graph. 3*, 2, 1–19.

ATKINSON, K. 1997. *The Numerical Solution of Integral Equations of the Second Kind*. Cambridge University Press.

BEYLKIN, G., COIFMAN, R., AND ROKHLIN, V. 1991. Fast wavelet transforms and numerical algorithms I. *Commun. Pure Appl. Math* 44, 141–183.

CARR, N. A., HALL, J. D., AND HART, J. C. 2003. GPU algorithms for radiosity and subsurface scattering. In *Proceedings of Graphics Hardware*. 51–59.

CHESLACK-POSTAVA, E., GOODNIGHT, N., NG, R., AND RAMAMOORTHI, R. 2007. 4D compression and relighting with high-resolution light transport matrices. In *Proceedings of ACM SIGGRAPH Symposium on Interactive 3D Graphics and Games*.

CHRISTENSEN, P. H. 2003. Adjoints and importance in rendering: An overview. *IEEE Trans. Visual. Comput. Grap. 9*, 3, 329–340.

CHRISTENSEN, P. H., LISCHINSKI, D., STOLLNITZ, E. J., AND SALESIN, D. H. 1997. Clustering for glossy global illumination. *ACM Trans. Graph. 16*, 1, 3–33.

CHRISTENSEN, P. H., STOLLNITZ, E. J., SALESIN, D. H., AND DEROSE, T. D. 1996. Global illumination of glossy environments using wavelets and importance. *ACM Trans. Graph. 15*, 1, 37–71.

CHUANG, Y.-Y., ZONGKER, D. E., HINDORFF, J., CURLESS, B., SALESIN, D. H., AND SZELISKI, R. 2000. Environment matting extensions: Towards higher accuracy and real-time capture. In *Proceedings of ACM SIGGRAPH*. Computer Graphics Proceedings, Annual Conference Series. 121–130.

COHEN, M. F., CHEN, S. E., WALLACE, J. R., AND GREENBERG, D. P. 1988. A progressive refinement approach to fast radiosity image generation. In *Proceedings of ACM SIGGRAPH (Computer Graphics)*. ACM Press, 75–84.

COHEN, M. F. AND WALLACE, J. R. 1993. *Radiosity and Realistic Image Synthesis*. Morgan Kaufmann.

DANA, K. J., VAN GINNEKEN, B., NAYAR, S. K., AND KOENDERINK, J. J. 1999. Reflectance and texture of real-world surfaces. *ACM Trans. Graph. 18*, 1, 1–34.

DEBEVEC, P., HAWKINS, T., TCHOU, C., DUIKER, H.-P., SAROKIN, W., AND SAGAR, M. 2000. Acquiring the reflectance field of a human face. In *Proceedings of ACM SIGGRAPH*. ACM Press, 145–156.

DOBASHI, Y., KANEDA, K., NAKATANI, H., AND YAMASHITA, H. 1995. A quick rendering method using basis functions for interactive lighting design. *Comp. Graph. For*, *14*, 3, 229–240.

DOBASHI, Y., KANEDA, K., YAMASHITA, H., AND NISHITA, T. 1996. Method for calculation of sky light luminance aiming at an interactive architectural design. *Comp. Graph. For. 15*, 3, 109–118.

DORSEY, J. O., ARVO, J., AND GREENBERG, D. 1995. Interactive design of complex time-dependent lighting. *IEEE Comp. Graph. Appli. 15*, 2, 26–36.

DUTRÉ, P. 1996. Mathematical frameworks and monte carlo algorithms for global illumination in computer graphics. Ph.D. thesis, Katholieke Universiteit Leuven.

DUTRÉ, P., BEKAERT, P., AND BALA, K. 2003. *Advanced Global Illumination*. AK Peters.

DUTRÉ, P., BEKAERT, P., SUYKENS, F., AND WILLEMS, Y. D. 1996. Bidirectional radiosity. In *Proceedings of Eurographics Workshop on Rendering*.

GARG, G., TALVALA, E.-V., LEVOY, M., AND LENSCH, H. P. A. 2006. Symmetric photography: Exploiting data-sparseness in reflectance fields. In *Proceedings of Eurographics Symposium on Rendering (Rendering Techniques)*. 251–262.

GERSHBEIN, R., SCHRDER, P., AND HANRAHAN, P. 1994. Textures and radiosity: controlling emission and reflection with texture maps. In *Proceedings of ACM SIGGRAPH (Computer Graphics)*. ACM Press, New York, NY, 51–58.

GOBBETTI, E., SPANÒ, L., AND AGUS, M. 2003. Hierarchical higher order face cluster radiosity for global illumination walkthroughs of complex non-diffuse environments. *Comp. Graph. For. 22*, 3, 563–572.

GOESELE, M., LENSCH, H. P. A., LANG, J., FUCHS, C., AND SEIDEL, H.-P. 2004. Disco: acquisition of translucent objects. *ACM Trans. Graph. 23*, 3, 835–844.

GORTLER, S. J., GRZESZCZUK, R., SZELISKI, R., AND COHEN, M. F. 1996. The lumigraph. In *Proceedings of SIGGRAPH*. 43–54.

GORTLER, S. J., SCHRDER, P., COHEN, M. F., AND HANRAHAN, P. 1993. Wavelet radiosity. In *Proceedings of ACM SIGGRAPH*. ACM Press, 221–230.

GREEN, P., KAUTZ, J., MATUSIK, W., AND DURAND, F. 2006. View-dependent precomputed light transport using nonlinear gaussian function approximations. In *Proceedings of ACM SIGGRAPH Symposium on Interactive 3D Graphics and Games*.

HANRAHAN, P., SALZMAN, D., AND AUPPERLE, L. 1991. A rapid hierarchical radiosity algorithm. In *Proceedings of ACM SIGGRAPH (Computer Graphics)*. ACM Press, 197–206.

HAO, X., BABY, T., AND VARSHNEY, A. 2003. Interactive subsurface scattering for translucent meshes. In *Proceedings of ACM SIGGRAPH Symposium on Interactive 3D Graphics*. 75–82.

HAO, X. AND VARSHNEY, A. 2004. Real-time rendering of translucent meshes. *ACM Trans. Graph. 23*, 2 (Apr.), 120–142.

HAŠAN, M., PELLACINI, F., AND BALA, K. 2006. Direct-to-indirect transfer for cinematic relighting. *ACM Trans. Graph. 25*, 3, 1089–1097.

HAWKINS, T., EINARSSON, P., AND DEBEVEC, P. 2005. A dual light stage. In *Proceedings of the Eurographics Symposium on Rendering (Rendering Techniques)*. 91–98.

HAWKINS, T., WENGER, A., TCHOU, C., GARDNER, A., GÖRANSSON, F., AND DEBEVEC, P. 2004. Animatable facial reflectance fields. In *Proceding of Eurographics Symposium on Rendering (Rendering Techniques)*. 309–320.

HECKBERT, P. S. 1991. Simulating global illumination using adaptive meshing. Ph.D. thesis, University of California, Berkeley.

IMMEL, D. S., COHEN, M. F., AND GREENBERG, D. P. 1986. A radiosity method for non-diffuse environments. In *Proceedings of ACM SIGGRAPH (Computer Graphics)*. ACM Press, 133–142.

JAMES, D. AND FATAHALIAN, K. 2003. Precomputing interactive dynamic deformable scenes. *ACM Trans. Graph.s 22*, 3, 879–887.

KAJIYA, J. T. 1986. The rendering equation. In *Proceedings of ACM SIGGRAPH (Computer Graphics)*. ACM Press, 143–150.

KAUTZ, J. AND MCCOOL, M. D. 1999. Interactive rendering with arbitrary brdfs using separable approximations. In *Proceedings of Eurographics Workshop on Rendering*. 281–292.

KAUTZ, J., SLOAN, P.-P., AND SNYDER, J. 2002. Fast, arbitrary brdf shading for low-frequency lighting using spherical harmonics. In *Proceedings of Eurographics Workshop on Rendering (Rendering Techniques)*. 301–308.

KONTKANEN, J., TURQUIN, E., HOLZSCHUCH, N., AND SILLION, F. 2006. Wavelet radiance transport for interactive indirect lighting. In *Proceedings of Eurographics Symposium on Rendering (Rendering Techniques)*. Eurographics Association.

KOUDELKA, M., MAGDA, S., BELHUMEUR, P. N., AND KRIEGMAN, D. J. 2003. Acquisition, compression, and synthesis of bidirectional texture functions. In *Proceedings of 3rd International Workshop on Texture Analysis and Synthesis*. 59–64.

KOUDELKA, M. L., BELHUMEUR, P. N., MAGDA, S., AND KRIEGMAN, D. J. 2001. Image-based modeling and rendering of surfaces with arbitrary brdfs. In *Conference on Computer Vision and Pattern Recognition (CVPR)*. Vol. 1. 568–575.

KRISTENSEN, A. W., AKENINE-MÖLLER, T., AND WANN JENSEN, H. 2005. Precomputed local radiance transfer for real-time lighting design. *ACM Trans. Graph. 24*, 3, 1208–1215.

KŘIVÁNEK, J., GAUTRON, P., PATTANAIK, S., AND BOUATOUCH, K. 2005. Radiance caching for efficient global illumination computation. *IEEE Trans. Visual. Comp. Graph. 11*, 5.

KŘIVÁNEK, J., PATTANAIK, S., AND ŽÁRA, J. 2004. Adaptive mesh subdivision for precomputed radiance transfer. In *Proceedings of the 20th Spring Conference on Computer Graphics (SCCG '04)*. ACM Press, 106–111.

LAFORTUNE, E. 1996. Mathematical models and monte carlo algorithms for physically based rendering. Ph.D. thesis, Katholieke Universiteit Leuven.

LAFORTUNE, E. P. AND WILLEMS, Y. D. 1994. A theoretical framework for physically based rendering. *Comp. Grap. For. 13*, 2.

LECOT, G., LEVY, B., ALONSO, L., AND PAUL, J.-C. 2005. Master-element vector irradiance for large tessellated models. In *Proceedings of GRAPHITE*.

LEHTINEN, J. AND KAUTZ, J. 2003. Matrix radiance transfer. In *Proceedings of ACM SIGGRAPH Symposium on Interactive 3D Graphics*. 59–64.

LEHTINEN, J., ZWICKER, M., KONTKANEN, J., TURQUIN, E., SILLION, F., AND AILA, T. 2007. Meshless finite elements for hierarchical global illumination. Tech. rep. TML-B7, Publications in Telecommunications Software and Multimedia, Helsinki University of Technology.

LENSCH, H. P. A., GOESELE, M., BEKAERT, P., KAUTZ, J., MAGNOR, M. A., LANG, J., AND SEIDEL, H.-P. 2003. Interactive rendering of translucent objects. *Comp. Graph. For. 22*, 2, 195–206.

LIU, X., SLOAN, P.-P., SHUM, H.-Y., AND SNYDER, J. 2004. All-frequency precomputed radiance transfer for glossy objects. In *Proceedings of the Eurographics Symposium on Rendering (Rendering Techniques)*. The Eurographics Association, 337–344.

MAHAJAN, D., KEMELMACHER SHLIZERMAN, I., RAMAMOORTHI, R., AND BELHUMEUR, P. 2007. A theory of locally low dimensional light transport. *ACM Trans. Graph. 26*, 3.

MALZBENDER, T., GELB, D., AND WOLTERS, H. 2001. Polynomial texture maps. In *Proceedings of ACM SIGGRAPH*. 519–528.

MASSELUS, V., PEERS, P., DUTRÉ, P., AND WILLEMS, Y. D. 2003. Relighting with 4D incident light fields. *ACM Trans. Graph. 22*, 3, 613–620.

MATUSIK, W., LOPER, M., AND PFISTER, H. 2004. Progressively-refined reflectance functions from natural illumination. In *Proceedings of Eurographics Symposium on Rendering (Rendering Techniques)*. 299–308.

MATUSIK, W., PFISTER, H., BRAND, M., AND MCMILLAN, L. 2003. A data-driven reflectance model. *ACM Trans. Graph. 22*, 3, 759–769.

MATUSIK, W., PFISTER, H., NGAN, A., BEARDSLEY, P., ZIEGLER, R., AND MCMILLAN, L. 2002. Image-based 3D photography using opacity hulls. *ACM Trans. Graph. 21*, 3, 427–437.

MATUSIK, W., PFISTER, H., ZIEGLER, R., NGAN, A., AND MCMILLAN, L. 2002. Acquisition and rendering of transparent and refractive objects. In *Proceedings of Eurographics Workshop on Rendering (Rendering Techniques)*. 267–278.

MILLER, G. S. P., RUBIN, S. M., AND PONCELEON, D. B. 1998. Lazy decompression of surface light fields for precomputed global illumination. In *Proceedings of Eurographics Workshop on Rendering (Rendering Techniques)*. 281–292.

MÜLLER, G., MESETH, J., AND KLEIN, R. 2003. Compression and real-time rendering of measured btfs using local pca. In *Proceedinds of Vision, Modeling and Visualisation*.

MÜLLER, G., MESETH, J., SATTLER, M., SARLETTE, R., AND KLEIN, R. 2005. Acquisition, synthesis, and rendering of bidirectional texture functions. *Comput. Graph. For. 24*, 1, 83–109.

NAYAR, S. K., BELHUMEUR, P. N., AND BOULT, T. E. 2004. Lighting sensitive display. *ACM Trans. Graph. 23*, 4, 963–979.

NG, R., RAMAMOORTHI, R., AND HANRAHAN, P. 2003. All-frequency shadows using non-linear wavelet lighting approximation. *ACM Trans. Graph. 22*, 3, 376–381.

NG, R., RAMAMOORTHI, R., AND HANRAHAN, P. 2004. Triple product wavelet integrals for all-frequency relighting. *ACM Trans. Graph. 23*, 3, 477–487.

NIMEROFF, J. S., SIMONCELLI, E., AND DORSEY, J. 1994. Efficient re-rendering of naturally illuminated environments. In *Proceedings of Eurographics Workshop on Rendering*. Darmstadt, Germany, 359–373.

OVERBECK, R., BEN-ARTZI, A., RAMAMOORTHI, R., AND GRINSPUN, E. 2006. Exploiting temporal coherence for incremental all-frequency relighting. In *Proceedings of Eurographics Symposium on Rendering (Rendering Techniques)*. Eurographics Association, 151–160.

PATTANAIK, S. N. AND MUDUR, S. P. 1995. Adjoint equations and random walks for illumination computation. *ACM Trans. Graph. 14*, 1, 77–102.

PEERS, P. AND DUTRÉ, P. 2003. Wavelet environment matting. In *Proceedings of Eurographics Symposium on Rendering (Rendering Techniques)*. 157–166.

PEERS, P. AND DUTRÉ, P. 2005. Inferring reflectance functions from wavelet noise. In *Proceedings of Eurographics Symposium on Rendering (Rendering Techniques)*. 173–182.

PETER, I. AND PIETREK, G. 1998. Importance driven construction of photon maps. In *Proceedings of Eurographics Workshop on Rendering*. 269–280.

SEN, P., CHEN, B., GARG, G., MARSCHNER, S. R., HOROWITZ, M., LEVOY, M., AND LENSCH, H. P. A. 2005. Dual photography. *ACM Trans. Graph. 24*, 3, 745–755.

SILLION, F. X. 1995. A unified hierarchical algorithm for global illumination with scattering volumes and object clusters. *IEEE Trans. Visualiz. Comput. Graph. 1*, 3, 240–254.

SILLION, F. X., ARVO, J. R., WESTIN, S. H., AND GREENBERG, D. P. 1991. A global illumination solution for general reflectance distributions. In *Proceedings of ACM SIGGRAPH 91 (Computer Graphics)*. ACM Press, 187–196.

SLOAN, P.-P., HALL, J., HART, J., AND SNYDER, J. 2003. Clustered principal components for precomputed radiance transfer. *ACM Trans. Graph. 22*, 3, 382–391.

SLOAN, P.-P., KAUTZ, J., AND SNYDER, J. 2002. Precomputed radiance transfer for real-time rendering in dynamic, low-frequency lighting environments. *ACM Trans. Graph. 21*, 3, 527–536.

SLOAN, P.-P., LIU, X., SHUM, H.-Y., AND SNYDER, J. 2003. Bi-scale radiance transfer. *ACM Trans. Graph. 22*, 3, 370–375.

SLOAN, P.-P., LUNA, B., AND SNYDER, J. 2005. Local, deformable precomputed radiance transfer. *ACM Trans. Graph. 24*, 3, 1216–1224.

SMITS, B., ARVO, J., AND GREENBERG, D. 1994. A clustering algorithm for radiosity in complex environments. In *Proceedings of ACM SIGGRAPH*. ACM Press, 435–442.

SMITS, B. E., ARVO, J. R., AND SALESIN, D. H. 1992. An importance-driven radiosity algorithm. In *Proceedings of ACM SIGGRAPH (Computer Graphics)*. ACM Press, 273–282.

SUN, W. AND MUKHERJEE, A. 2006. Generalized wavelet product integral for rendering dynamic glossy objects. *ACM Trans. Graph. 25*, 3, 955–966.

TEO, P., SIMONCELLI, E., AND HEEGER, D. 1997. Efficient linear re-rendering for interactive lighting design. Tech. rep. CS-TN-97-60, Stanford University.

TSAI, Y.-T. AND SHIH, Z.-C. 2006. All-frequency precomputed radiance transfer using spherical radial basis functions and clustered tensor approximation. *ACM Trans. Graph. 25*, 3, 967–976.

VASILESCU, M. A. O. AND TERZOPOULOS, D. 2004. Tensortextures: multilinear image-based rendering. *ACM Trans. Graph. 23*, 3, 336–342.

VEACH, E. 1997. Robust monte carlo methods for light transport simulation. Ph.D. thesis, Stanford University.

VEACH, E. AND GUIBAS, L. J. 1997. Metropolis light transport. In *Proceedings of ACM SIGGRAPH*. 65–76.

WANG, L., WANG, W., DORSEY, J., YANG, X., GUO, B., AND SHUM, H.-Y. 2005. Real-time rendering of plant leaves. *ACM Trans. Graph. 24*, 3, 712–719.

WANG, R., NG, R., LUEBKE, D., AND HUMPHREYS, G. 2006. Efficient wavelet rotation for environment map rendering. In *Proceedings of Eurographics Symposium on Rendering (Rendering Techniques)*. 173–182.

WANG, R., TRAN, J., AND LUEBKE, D. 2004. All-frequency relighting of non-diffuse objects using separable brdf approximation. In *Proceedings of the Eurographics Symposium on Rendering (Rendering Techniques)*. The Eurographics Association, 345–354.

WANG, R., TRAN, J., AND LUEBKE, D. 2005. All-frequency interactive relighting of translucent objects with single and multiple scattering. *ACM Trans. Graph. 24*, 3, 1202–1207.

WANG, R., TRAN, J., AND LUEBKE, D. 2006. All-frequency relighting of glossy objects. *ACM Trans. Graph. 25*, 2, 293–318.

WANN JENSEN, H. 1996. Global illumination using photon maps. In *Proceedings of Eurographics Workshop on Rendering 1996*. Springer-Verlag, 21–30.

WARD, G. J., RUBINSTEIN, F. M., AND CLEAR, R. D. 1988. A ray tracing solution for diffuse interreflection. In *Proceedings of SIGGRAPH 88 (Computer Graphics)*. 85–92.

WENGER, A., GARDNER, A., TCHOU, C., UNGER, J., HAWKINS, T., AND DEBEVEC, P. 2005. Performance relighting and reflectance transformation with time-multiplexed illumination. *ACM Trans. Graph. 24*, 3, 756–764.

WEYRICH, T., PFISTER, H., AND GROSS, M. 2005. Rendering deformable surface reflectance fields. *IEEE Trans. Visual. Comput. Graph. 11*, 1, 48–58.

WILLMOTT, A., HECKBERT, P., AND GARLAND, M. 1999. Face cluster radiosity. In *Proceedings of Eurographics Workshop on Rendering*.

WONG, T.-T., HENG, P.-A., AND FU, C.-W. 2001. Interactive relighting of panoramas. *IEEE Comput. Graph. Appl. 21*, 2, 32–41.

WONG, T.-T., HENG, P.-A., OR, S.-H., AND NG, W.-Y. 1997. Image-based rendering with controllable illumination. In *Proceedings of Eurographics Workshop on Rendering*. 13–22.

ZHOU, K., HU, Y., LIN, S., GUO, B., AND SHUM, H.-Y. 2005. Precomputed shadow fields for dynamic scenes. *ACM Trans. Graph. 24*, 3, 1196–1201.

ZONGKER, D. E., WERNER, D. M., CURLESS, B., AND SALESIN, D. H. 1999. Environment matting and compositing. In *Proceedings of SIGGRAPH*. Computer Graphics Proceedings, Annual Conference Series. 205–214.

Received November 2005; revised May 2007; accepted August 2007